JNC TN9400 2002-063

Effects of Existing Evaluated Nuclear Data Files on Neutronics Characteristics of the BFS-62-3A Critical Assembly Benchmark Model

November 2002

O-ARAI ENGINEERING CENTER
JAPAN NUCLEAR CYCLE DEVELOPMENT INSTITUTE

〒319-1184　茨城県那珂郡東海村村松４番地４９
核燃料サイクル開発機構
技術展開部　技術協力課

Inquiries about copyright and reproduction should be addressed to　:
Technical Cooperation Section,
Technology Management Division,
Japan Nuclear Cycle Development Institute
4-49, Muramatsu, Tokai-mura, Naka-gun, Ibaraki　319-1184,　JAPAN

JNC TN9400 2002-063
November 2002

Effects of Existing Evaluated Nuclear Data Files on Neutronics Characteristics of the BFS-62-3A Critical Assembly Benchmark Model

Mikhail SEMENOV *)

ABSTRACT

This report is continuation of studying of the experiments performed on BFS-62-3A critical assembly in Russia. The objective of work is definition of the cross section uncertainties on reactor neutronics parameters as applied to the hybrid core of the BN-600 reactor of Beloyarskaya NPP.

Two-dimensional benchmark model of BFS-62-3A was created specially for these purposes and experimental values were reduced to it. Benchmark characteristics for this assembly are 1) criticality; 2) central fission rate ratios (spectral indices); and 3) fission rate distributions in stainless steel reflector.

The effects of nuclear data libraries have been studied by comparing the results calculated using available modern data libraries - ENDF/B-V, ENDF/B-VI, ENDF/B-VI-PT, JENDL-3.2 and ABBN-93. All results were computed by Monte Carlo method with the continuous energy cross sections.

The checking of the cross sections of major isotopes on wide benchmark criticality collection was made.

It was shown that ENDF/B-V data underestimate the criticality of fast reactor systems up to 2% Δk. As for the rest data, the difference between each other in criticality for BFS-62-3A is around 0.6% Δk. However, taking into account the results obtained for other fast reactor benchmarks (and steel-reflected also), it may conclude that the difference in criticality calculation results can achieve 1% Δk. This value is in a good agreement with cross section uncertainty evaluated for BN-600 hybrid core ($\pm$0.6%Δk).

This work is related to the JNC-IPPE Collaboration on Experimental Investigation of Excess Weapons Grade Pu Disposition in BN-600 Reactor Using BFS-2 Facility.

KEY WORDS: BFS-62-3A, benchmark model, MCNP code, MMKKENO code, continuous energy, criticality benchmarks, experimental data, MOX fuel, steel reflector.

---

*) JNC International Fellow (10/12/2001 - 9/12/2002)
Reactor Physics Research Group, System Engineering Technology Division, O-arai Engineering Center, JNC, Japan.

JNC TN9400 2002-063
2002 年 11 月

BFS-62-3A 炉心ベンチマークモデルの核特性に関する既存核データライブラリの影響

（研究報告書）

ミハイル　セミョノフ*

要　旨

本報告書は, ロシアの臨界実験施設 BFS-2 で実施された BFS-62-3A 体系に関する検討結果の続報である。目的は，ロシアの高速発電所 BN-600 のハイブリッド炉心に関係する核特性に対して，断面積に基づく不確かさを評価することである。

BFS-62-3A 体系の２次元ベンチマーク用モデルを作成するとともに，本モデルに対する実験値を算出した。評価した核特性は，臨界性，炉中心核分裂反応率比（スペクトルインデックス）及び鋼製反射体領域の核分裂反応率分布である。

核データライブラリによる差異を，ENDF/B-V，ENDF/B-VI，ENDF/B-VI-PT，JENDL-3.2 及び ABBN-93 を適用した解析値を比較することにより調べた。解析はすべて連続エネルギーモンテカルロ手法で行った。

ENDF/B-V は高速炉の臨界性を 2%Δk 過小評価すること, ENDF/B-V 以外のライブラリが臨界性に及ぼす差異は約 0.6%Δk であることがわかった。しかし，鋼製反射体付き体系を含む他の高速炉ベンチマーク体系の解析結果も考慮し, 臨界性に関するライブラリ間の差は 1%Δk 程度であると結論した。この値は，BN-600 ハイブリッド炉心の断面積に基づく不確かさ（±0.6%Δk）と良く一致している。

なお，本研究は，ロシア余剰核兵器解体プルトニウム処分協力のために実施しているロシア物理エネルギー研究所(IPPE）の BFS-2 臨界実験装置を利用した JNC-IPPE 共同研究に関連して実施したものである。

キーワード：BFS-62-3A，ベンチマークモデル，MCNP コード，MMKKENO コード，連続エネルギー，臨界性ベンチマーク，実験データ，MOX 燃料，鋼製反射体

---

*: 大洗工学センター　システム技術開発部　中性子工学グループ
国際特別研究員（2001 年 12 月 10 日～2002 年 12 月 9 日）

CONTENTS

LIST OF TABLES

LIST OF FIGURES

1. INTRODUCTION

In definition of neutronics characteristics either for conventional UOX or for MOX reactor core, one of the main targets is the estimation of the accuracy of the calculated characteristics. Unfortunately, the nuclear data provide the main uncertainty in calculation of physics characteristics for MOX core. So the definition and estimation of the calculation uncertainty caused by nuclear data is one of the key points and is being required. One of the ways for that is the studying of influence of different nuclear data libraries on nuclear characteristics of the fast reactor with MOX fuel.

I decided to apply for such investigations the well-known method, based on studying of the simple benchmark-model characteristics.

This report describes simple calculation benchmark-model of the BFS-62-3A assembly (BN-600 mock-up hybrid core) and presents the experimental values transformed for this model. Benchmark characteristics for this assembly are 1) criticality; 2) central fission rate ratios (spectral indices); and 3) fission rate distributions in stainless steel reflector.

The calculation results obtained by using available modern data libraries (ENDF/B-V, ENDF/B-VI, ENDF/B-VI-PT, JENDL-3.2 and ABBN-93) are presented also. All results were computed by Monte Carlo method.

In addition to BFS-62-3A benchmark, a big list of international criticality benchmarks, which include small systems, fast reactor assemblies and special benchmarks with steel reflector, were investigated.

2. DETAILED DESCRIPTION

2.1 Overview of Experiments

The Big Physical Test Bench (BFS-2) fast critical facility was built at the Institute for Physics and Power Engineering (IPPE) site in Obninsk (Russia) in 1969 to obtain neutron physics information necessary for the design of large fast reactors with a unit power up to 3000 MWe. The vessel, in which the investigated critical assemblies are constructed, has an effective diameter ~5 meters and a height ~3.3 meters. For simulating in-vessel storages, shielding and screens, there is so called metal column in the vessel part.

The BFS-62-3A Assembly was part of a series of five criticality mock-up cores built in Assembly 62 of the BFS-2 facility to provide data for verification of the accuracy of analysis system (calculation codes and neutron data) for the design of BN-600 (Russian commercial fast reactor) hybrid core.

The assemblies were uranium (or, partially stainless steel) reflected and had core fuel compositions containing different mixtures of uranium and plutonium. The first of these configurations, BFS-62-1, was built with only uranium fuel to model present state of the BN-600 reactor. Then enriched plutonium was progressively substituted for uranium in Phases 62-3A through 62-5. Experiments in Assemblies 62 were performed between 1999 and 2001.

The BFS Assembly 62-3A was designed to have mock-up experiments on BN-600 hybrid core.

Three nuclides, ^{235}U, ^{238}U and ^{239}Pu dominated the neutronic behavior in the core region. The core isotopic composition was close enough to reactor core. Thus, the spectrums for reactor core regions are very similar to assembly ones practically in all energy range. The comparison between two spectrums for MOX core region is presented on Fig. 1.

A very accurate transformation to a simplified model is needed to make the BFS-62-3A assembly a practical reactor benchmark, because there is simply too much geometric detail in an exact model of the assembly.

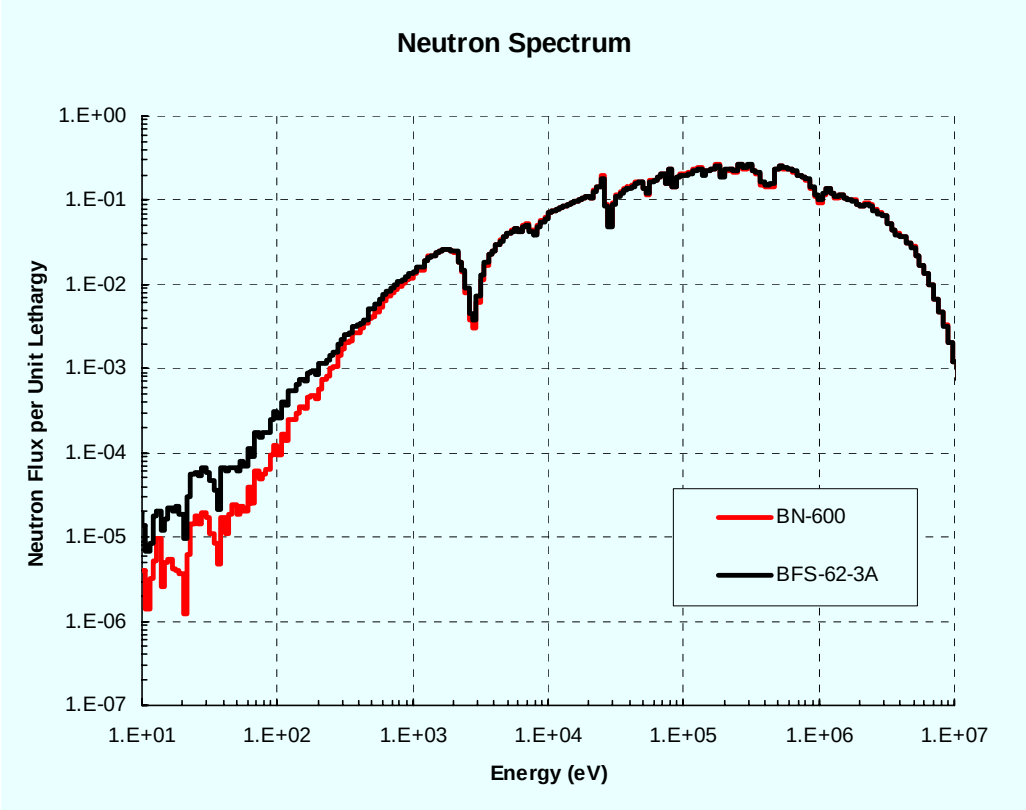

Fig. 1. Neutron spectrums for MOX core region

The transformation must reduce the detail to a practical level without masking any of the important features of the criticality experiment. And it must do this without increasing the total uncertainty far beyond that of the original experiment. Such a transformation is described in Section 3. It was made using a pair of multi-group Monte Carlo calculations. First, Assembly 62-3A was modeled in full detail - every pellet, stick, tube, and air gap was modeled explicitly. Then the region-wise compositions and volumes from this model were converted to a homogeneous, two-dimensional (RZ) model. This simple model is the criticality benchmark model. The difference in k_{eff} values from the two models was used to adjust the measured excess reactivity of Assembly 62-3A, yielding a result for the benchmark model. Uncertainties associated with this simplification, which go beyond Monte Carlo statistical uncertainties, were taken into account.

I hope, the BFS-62-3A assembly will be determined to be an acceptable criticality benchmark experiment.

2.2 Description of Experimental Configuration

As already mentioned, BFS-62-3A was the third of a series of five, uranium-steel-reflected, critical configurations built in BFS-2 with core compositions containing different mixtures of uranium and plutonium fuel. All five configurations had approximately the same core volume which approximated a cylinder of about 104 cm height and a stepped radial boundary of about 105 cm effective radius. Five different plate-type cells were used to vary the fuel composition in assemblies 62-1 to 62-5. The fuel compositions were varied by replacing the initial loading of enriched uranium pellets with combinations of 95%-enriched plutonium pellets and depleted uranium pellets. The sodium remained constant. A thick shield of depleted uranium was used throughout the series of configurations to produce a calculable model without requiring significant corrections for “room-return” neutrons. The outer core thickness was adjusted to make each phase critical.

In the approach to critical, the inverse count rate was monitored as the thickness of the outer core was increased. The control rods were in the least reactive (negative) position at this stage. The goal was to build a configuration that was within +0.10~+0.15 $ of critical when all the rods were moved to the most reactive position. The reactivity of the BFS-62-3A reference critical configuration was obtained from an inverse kinetics analysis of the power history when the fuel control and safety rods were fully inserted. The measured excess reactivity was 0.11 $ /1/.

The natural measurement unit, dollar, is related to k_{eff} by the expression, $\$=(\Delta k_{eff}/k_{eff})/\beta_{eff}$. Accordingly, knowledge of β_{eff} is needed to express the measurement in terms of k_{eff}. A value of 0.00623 was calculated for β_{eff} using ABBN-93.1 neutron cross-sections and delayed neutron data, along with HEX-Z model of BFS-62-3A. The forward and adjoint fluxes were computed with the TRIGEX code that then computed the kinetics parameters, including β_{eff}.

The BFS-62-3A assembly “reference” configuration was achieved on March 2000. This configuration had a total of 450 kg ^{239}Pu; 1,360 kg ^{235}U; 9,100 kg ^{238}U; 1,380 kg Na and Al; and 5,510 kg stainless steel. The result of the excess reactivity measurement was obtained at a room temperature.

A lot of details must be presented to describe precisely the as-built assembly. In fact, the task of modeling the exact pellet-by-pellet loading is very hard to do by hand. However, readers interested only in using the benchmark model need not be concerned with any of these details, since Section 3 contains a complete specification of the criticality benchmark model.

2.2.1 The BFS-2 Facility - Stainless steel cylindrical tubes, nominally 1 mm thick, 50 mm on a side (outside dimension) and 3.2 m long, were stacked vertically on diagrid plate.

The desired average composition was achieved by loading the tubes containing pellets of different materials such as depleted or enriched uranium; stainless steel; sodium, etc. The pellets were bare material or had a cladding. Figure 2 is an illustration of the pellets inside the tubes forming a unit cell for a particular region in a particular loading.

Fig. 2. Photograph of typical pellet-loaded BFS-62-3A tube

2.3 Description of Material Data

The composition data here were taken from working documents /2/.

3. BENCHMARK SPECIFICATIONS

3.1 Description of Model

Even the most casual perusal of Section 2 makes it clear that BFS-62-3A is much too complicated to be a practical criticality benchmark model without a great amount of simplification. Fortunately, it is possible to eliminate virtually all of the complexity, yielding a simple benchmark model, without losing any of the essential physics. Furthermore, this can be done without compromising the high accuracy of the experiment.

This was accomplished by computing the transformation from the detailed as-built experiment model to the simple benchmark model using the MMKKENO multi-group Monte Carlo code. Note that the term “transformation” will be used repeatedly through Section 3 and will, in all cases, refer to both the simplification of the model from the as-built plate-wise heterogeneous experiment model to the homogeneous cylindrical benchmark model, and also the correction of k_{eff} to account for these simplifications. MMKKENO eigenvalue calculations were made for the as-built model and for the benchmark model. The k_{eff} correction is simply the difference in k_{eff} between the two models.

The modeling of all the experimental detail was made by hand. Special computer code, which can reads an electronic database containing a description of the BFS assemblies and then to generate the MMKKENO input file for the as-built model, is creating at IPPE now, but unfortunately this work not finished yet. Therefore, each step of the modeling was checked very carefully by special graphical code. The values of Avogadro’s number and the atomic masses were made to conform to the values recommended by the ICSBEP /3/.

The key features retained in the benchmark model are the region-averaged compositions, region volumes, and the global RZ geometry. The geometry is depicted in Figure 3. The radial dimensions of the benchmark model are determined by the total cross-sectional area of the tube positions included in each region, i.e., radii of cylindrical boundaries conserve cross-sectional areas of the corresponding regions in the detailed model. Axial dimensions of each region were slightly adjusted to inner core heights.

Masses of the constituents within these regions are then homogenized to produce the region-averaged compositions, thereby conserving material masses within each region.

The plate heterogeneity effects, which would require much effort to capture accurately in effective homogenized cross sections in a deterministic modeling approach, are included in the Monte Carlo-calculated Δk of the transformation.

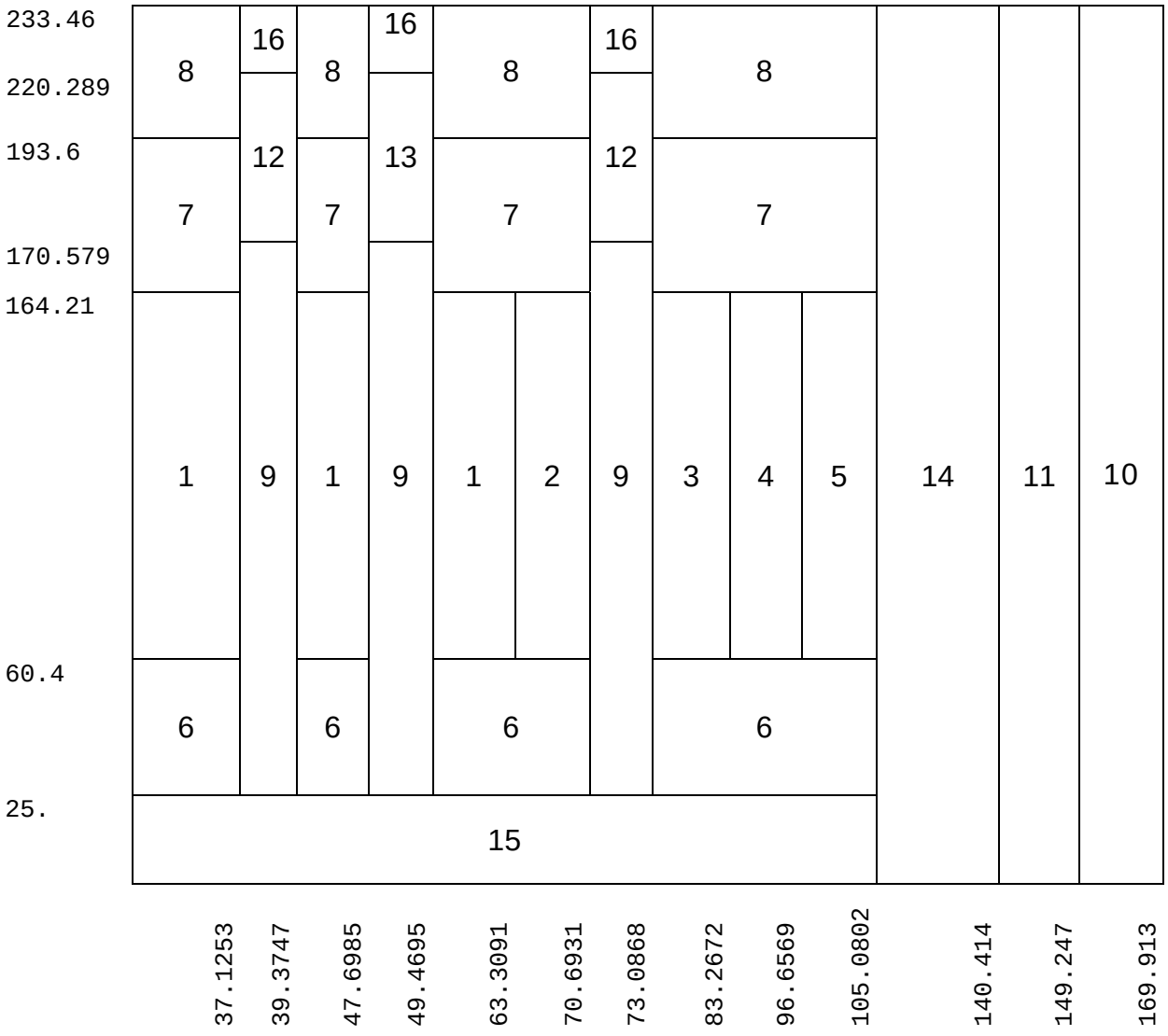

Figure 3. Benchmark-model geometry for BFS-62-3A (all sizes are given in cm)

The homogeneous cylindrical benchmark model resulting from the transformation of the as-built plate-wise heterogeneous BFS-62-3A is defined in the remainder of the section.

3.2 Dimensions

The benchmark model for BFS-62-3A can be modeled as 13 concentric cylindrical regions - containing the core with control and safety rod rings, surrounded by a thick cylindrical stainless steel reflector, surrounded by a concentric cylindrical boron shield region, surrounded by a final cylindrical depleted uranium region. The full configuration selected for the simplified benchmark model of BFS-62-3A contains 16 regions as shown in Figure 3.

Dimensions for all of these boundaries are given in cm in Figure 3.

3.3 Material Data

Table 1 contains the region-dependent composition data for the sixteen regions of the benchmark model. The masses of ^{241}Pu and ^{241}Am correspond to March 2000.

Table 1. Compositions of the benchmark-model regions (atoms/barn-cm)

Nuclide	Region 1 Inner Core 1	Region 2 Inner Core 2	Region 3 Middle Core	Region 4 MOX Core	Region 5 Outer Core
H	1.4530E-05	1.5820E-05	5.0247E-06	5.4267E-06	1.0623E-05
Na	6.5728E-03	6.5728E-03	6.2598E-03	5.6338E-03	5.6338E-03
C	3.0251E-04	3.0195E-04	4.0190E-04	4.2824E-04	3.6591E-04
Al	5.0165E-03	5.0196E-03	2.4161E-03	2.5889E-03	4.0036E-03
Ti	1.2084E-04	1.1997E-04	1.3688E-04	1.3838E-04	1.3132E-04
Cr	3.1741E-03	3.1507E-03	3.6349E-03	3.6993E-03	3.4462E-03
Mn	2.5034E-04	2.4850E-04	2.8976E-04	2.9177E-04	2.7457E-04
Fe	1.1510E-02	1.1467E-02	1.3168E-02	1.3410E-02	1.2513E-02
Ni	1.4841E-03	1.4732E-03	1.7017E-03	1.7297E-03	1.6133E-03
^{235}U	1.0642E-03	1.2222E-03	1.4786E-03	2.9720E-05	1.8646E-03
^{238}U	6.5656E-03	6.8447E-03	6.7585E-03	7.1145E-03	7.0132E-03
^{16}O	1.3199E-02	1.3282E-02	1.3240E-02	1.4299E-02	1.4148E-02
^{239}Pu	-	-	-	1.4501E-03	-
^{240}Pu	-	-	-	7.0234E-05	-
^{241}Pu[(a)]	-	-	-	8.0423E-07	-
^{241}Am[(a)]	-	-	-	2.9419E-06	-
Ga	-	-	-	8.7691E-05	-

(a) Masses of 241Pu and 241Am correspond to March 2000.

Table 1 (cont'd). Compositions of the benchmark-model regions

Nuclide	Region 6 Low Axial Blanket	Region 7 Upper Axial Blanket	Region 8 Upper Axial Shield	Region 9 Control Rod Follower	Region 10 Radial Blanket
H	2.4569E-04	7.0993E-06	3.5320E-04	-	1.0700E-05
Na	5.5007E-03	5.5276E-03	8.1420E-03	1.0936E-02	-
C	4.9780E-04	4.9949E-04	2.0820E-04	1.6468E-04	6.9662E-04
Al	3.1458E-03	3.1570E-03	7.8779E-04	6.2311E-04	4.5454E-03
Ti	8.6518E-05	8.6577E-05	3.2381E-04	2.5612E-04	4.3066E-05
Cr	2.3130E-03	2.3146E-03	8.6569E-03	6.8472E-03	1.1513E-03
Mn	1.8243E-04	1.8255E-04	6.8278E-04	5.4004E-04	9.0806E-05
Fe	8.4695E-03	8.4758E-03	3.1089E-02	2.4590E-02	4.3813E-03
Ni	1.0815E-03	1.0822E-03	4.0478E-03	3.2016E-03	5.3834E-04
^{235}U	3.8735E-05	3.8880E-05	-	-	5.8599E-05
^{238}U	9.2725E-03	9.3072E-03	-	-	1.4028E-02
^{16}O	1.8636E-02	1.8706E-02	-	-	2.8194E-02

Table 1 (cont'd). Compositions of the benchmark-model regions

Nuclide	Region 11 Boron Shield	Region 12 Control Rod	Region 13 Safety Rod
Na	-	9.8043E-03	-
C	1.1414E-02	6.0934E-03	1.5003E-02
Al	1.0477E-04	2.4029E-04	1.7229E-04
Ti	4.3066E-05	9.8771E-05	7.0817E-05
Cr	1.1513E-03	2.6405E-03	1.8932E-03
Mn	9.0806E-05	2.0826E-04	1.4932E-04
Fe	4.1347E-03	9.4828E-03	6.7990E-03
Ni	5.3834E-04	1.2347E-03	8.8523E-04
^{10}B	9.0632E-03	4.8000E-03	1.1907E-02
^{11}B	3.6481E-02	1.9320E-02	4.7925E-02

Table 1 (cont'd). Compositions of the benchmark-model regions

Nuclide	Region 14 Steel Reflector	Region 15 Support	Region 16 Upper Tube
C	2.4180E-04	9.2259E-05	4.5532E-05
Al	9.1493E-04	3.4909E-04	1.7229E-04
Ti	3.7607E-04	1.4349E-04	7.0817E-05
Cr	1.0054E-02	3.8361E-03	1.8932E-03
Mn	7.9296E-04	3.0256E-04	1.4932E-04
Fe	3.6106E-02	1.3776E-02	6.7990E-03
Ni	4.7010E-03	1.7937E-03	8.8523E-04

3.4 Temperature Data

The average temperature of BFS-62-3A during the criticality measurement was approximately room temperature. No temperature adjustment was made to the measured excess reactivity.

3.5 Experimental and Benchmark-Model k_{eff}

The transformation Δk (bias) from the as-built configuration to the benchmark model that was described in Section 3.1 was calculated using the MMKKENO multi-group Monte Carlo code with ABBN-93.1 data as given in Table 2. The calculations used 10,000 neutron histories per generation and 2,000 active generations after skipping 10. The uncertainties shown are just the statistical standard deviations from MMKKENO. It is noted that the combined uncertainties (± 0.00016) from the difference of the two Monte Carlo calculations is small relative to the transformation Δk (-0.01045) for this configuration.

Table 2. Eigenvalues for transformation from as-built model to RZ benchmark model [(a)]

	As-Built-Model k_{eff}	RZ Benchmark-Model k_{eff}	Transformation Δk (Bias)
MMKKENO (ABBN-93.1)	1.00163 ± 0.00011	0.99118 ± 0.00011	-0.01045 ± 0.00016

(a) Calculated using MMKKENO with ABBN-93.1 data.

An estimate of the total uncertainty in the transformation Δk from the as-built plate-wise heterogeneous critical-assembly model to the homogeneous cylindrical model is needed. Since there are no significant geometric approximations in the as-built model and there are no cross section processing approximations associated with either model, the only sources of uncertainty added to the original experimental uncertainty come from the Monte Carlo statistical precision and the sensitivity of the calculated Δk values to uncertainties in the basic cross section data. The major uncertainties in the assembly arise from fission production and absorption in ^{235}U, ^{238}U and ^{239}Pu and from transport cross section of Fe. Uncertainties in the k_{eff} of BN-600 reactor with different cores due to calculations with ABBN-93.1 data have been quantified and these values are approximately 1.5% /4/. Taking into account that sensitivity coefficients of BFS-62-3A are very similar to BN-600 hybrid core ones /5/, the uncertainty resulting from nuclear data for this assembly is 1.5%.

The issue is the uncertainty in the translation from the heterogeneous assembly model to the homogenous benchmark model. Because there is a strong correlation between the two calculations, the difference of the two calculations can have a much smaller uncertainty than either calculation. That is, the calculations for the transformation Δk value are based on the same code and on the same cross sections, with similar sensitivities of k_{eff} to the cross sections, and are thus highly correlated. The ensuing uncertainty in the transformation Δk is therefore assumed smaller by an order of magnitude, or ±0.15% Δk. Adding in quadrature the uncertainties due to use of ABBN-93.1 cross sections and the uncertainty of 0.02% from statistics in the two MMKKENO calculations yields a total uncertainty in the transformation Δk of 0.15% Δk.

This uncertainty estimate is believed to be conservative but still sufficiently small for criticality benchmark purposes. The actual correlations are likely higher than the values assumed in deriving the estimated uncertainty.

All the data for the experimental and benchmark-model k_{eff} values are summarized in Table 3. The data in the table are in units of k_{eff}. The experimental uncertainties affecting criticality would been divided into three broad categories. They are the uncertainties associated with 1) measurement technique, 2) geometry, and 3) compositions. Each category should be considered in turn and then the combined experimental uncertainty may be estimated. However, I have not possibility to do this work now, because uncertainties associated with geometry and composition data of some pellets not reported in full volume yet. So, benchmark-model uncertainty is not final.

Table 3. Experimental and benchmark-model eigenvalues [(a)]

Experimental k_{eff}	1.0007 ±
Monte Carlo transformation of model	-0.01045 ± 0.0015
Benchmark-Model k_{eff}	0.99025 ± 0.0015[(b)]

(a) Each uncertainty estimate is one standard deviation.
(b) Without of the total experimental uncertainty

3.6 Another Experimental Data

3.6.1 Central Spectral Indices

Detailed unit-cell measurements of the fission in ^{235}U and fission in ^{238}U and ^{239}Pu were made. Experimental results on fission cross-section ratios were obtained by the small size fission chambers using calibration method in the thermal column. Fission chambers were located in the inter-tube space. In the course of tests, these chambers were moved by means of manipulator vertically with a step from 5 to 10 mm along the central cell axis. Thus, as a result of measurements, actual cell-averaged values of the reaction rates could be obtained. Measurements in the core and calibration carried out

in thermal (graphite) column were repeated. The uncertainty of measurement of F239/F235 in the core is 1.5% and F238/F235 - 2%. F238 / F235 means fission of uranium-238 divided on fission of uranium-235, etc.

The details of the technique used for counting the activated foils and reducing the data to absolute reaction rates were expounded in /6/.

The measured reaction rate ratios are given in Table 4 along with calculated correction factors (to be applied to the measured values) for heterogeneities and final benchmark-results. The heterogeneous corrections were computed with the one-dimensional plate model by the FFCP code using first flight collision probability method taking into account the resonance effects based on the sub-group approach. The model used to represent the unit cell in this problem is described in /7/.

Table 4. Experimental and benchmark-model spectral indices

	Measurement	Calculated Heterogeneity Correction Factors	Benchmark-Results
F239 / F235	0.937	1.007	0.944
F238 / F235	0.0202	1.053	0.0213

3.6.2 Radial Fission Rate Distributions

The effect of stainless steel reflector that replaced UO_2 blanket in the peripheral on the fission reaction rate distribution results in increasing the power heating in the radial reflector. Clarification of the problem is quite urgent from the viewpoint of analysis accuracy estimation of the neutron irradiation of irremovable reactor constructions, neutron fluxes on control devices, etc. As for the fuel region, mean values and the standard deviation values show that the analysis accuracy is almost same level as the measurement uncertainty /8/. So, I decided to limit the consideration of this problem only to steel reflector.

Distribution of ^{235}U, ^{238}U and ^{239}Pu fission reaction rates was measured also by the small size fission chambers located in the inter-tube space at the level of the core

midplane from core center to stainless steel reflector direction. The uncertainty of measurement of fission rates of ^{235}U and ^{239}Pu in the core is 1.5-2%. For ^{238}U, experimental error is some higher, namely: 2-3%. The experimental uncertainties not clear reported for stainless steel region but I suppose that this value isn't better than 5~7% (it is an optimistical estimation).

Transformation of measurement results had a few steps. First of all, the heterogeneous correction factors were determined for all investigated cross sections in the core center position. Heterogeneous corrections were determined separately by using FFCP and heterogeneous cross sections were defined not over cell height but only over fission chamber height, i.e. ±2 cm around core midplane. Then flux corrections were computed which take into account difference between total flux distribution in real configuration and benchmark one. This procedure was done by using the TRIGEX code in diffusion approximation. Moreover, experimental positions in steel reflector were shifted on 1.6287 cm to take into account real distance between core boundary and measurement points. Benchmark results were determined like:

$$E^* = \frac{E \times C_F}{C_H}, \text{ where}$$

E^* - benchmark result;

E – experimental value;

C_F – flux correction;

C_H – heterogeneous correction.

After that, all measurement points were normalized on core center value. Benchmark results are given in Tables 5~7 along with experimental values and correction factors ones.

Table 5. ^{235}U fission rate distribution

R, cm	E	C_F	C_H	Benchmark-Results (Normalized)
Center	0.993	1.0484	0.997	-
110.5747	0.725	1.0048	1.000	0.6976
119.4082	0.710	1.0065	1.000	0.6844
128.2416	0.547	1.000	1.000	0.5238
137.0750	0.272	0.9967	1.000	0.2596

Table 6. ^{239}Pu fission rate distribution

R, cm	E	C_F	C_H	Benchmark-Results (Normalized)
Center	0.994	1.0484	1.003	-
110.5747	0.750	1.0048	1.000	0.7253
119.4082	0.744	1.0065	1.000	0.7207
128.2416	0.575	1.000	1.000	0.5534
137.0750	0.289	0.9967	1.000	0.2772

Table 7. ^{238}U fission rate distribution

R, cm	E	C_F	C_H	Benchmark-Results (Normalized)
Center	1.007	1.0484	1.04	-
110.5747	0.2820	1.0048	1.000	0.2791
119.4082	0.1102	1.0065	1.000	0.1093
128.2416	0.0459	1.000	1.000	0.0452
137.0750	0.0199	0.9967	1.000	0.0195

4. RESULTS OF SAMPLE CALCULATIONS

4.1 Criticality

All calculations connected with creating of the benchmark model and reductions of the experimental results to this model were carried out by IPPE (Russian) standard neutronics calculation codes and cross sections. However, it was very interesting to compare obtained results with another neutron data libraries existing on today. I had a possibility to make calculations with ENDF/B-V, ENDF/B-VI, ENDF/B-VI (with probability table treatment of the unresolved resonance region), and JENDL-3.2 files also. The calculations used 20,000 neutron histories per generation and 5,000 active generations after skipping 10.

Results of sample calculations of the benchmark model of BFS-62-3A are given in Table 8. A sample MCNP input listing for Version 4C of the MCNP code with the continuous energy 60c cross sections for all nuclides (i.e., ENDF/B-VI) is given in Appendix.

Table 8. Sample calculation results

Code (Cross Section Set) →	MCNP-4C (Continuous Energy ENDF/B-V)	MCNP-4C (Continuous Energy ENDF/B-VI)	MCNP-4C (Continuous Energy ENDF/B-VI-PT)[a)]
BFS-62-3A	0.96760±0.00005	0.98939±0.00005	0.99211±0.00005

a) Probability table

Table 8 (cont'd). Sample calculation results

Code (Cross Section Set) →	MCNP-4B (Continuous Energy JENDL-3.2)[a)]	MMKKENO (299-group ABBN-93.1)
BFS-62-3A	0.98661±0.00005	0.99118±0.00011

a) FSXJ32A2 binary library /9/

All calculation results (except ENDF/B-V) are in good agreement with each other and slightly (~+0.2-0.4% Δk) are differed from the benchmark k_{eff}. The maximum value

has ENDF/B-VI-PT and the minimum one has JENDL-3.2. The comparison between ENDF/B-VI data indicates the probability table treatment of the unresolved resonance region has not very big (~0.3% Δk) effect in calculations for this assembly – an expected conclusion for a fast reactor system. The distinction for the MCNP result with ENDF/B-V data from the benchmark k_{eff} is very large. Most probably, the effect closely connected with low threshold of unresolved resonance region for main fuel isotopes in this library.

4.2 Central Spectral Indices

To calculate these parameters, I picked out special subzone in the core center (10 cm OD and 8 cm height). MCNP tallies were used to calculate ^{235}U, ^{238}U and ^{239}Pu fission rates in this region. The calculations used 20,000 neutron histories per generation and 5,000 active generations after skipping 10. The statistical errors are very negligible (not more than 0.5%) and much less than experimental uncertainties (~2%).

Results of calculations of the spectral indices of BFS-62-3A and the comparison with the benchmark values are given in Table 9.

Table 9. Sample calculation results

	$E_{benchmark}$	B-V	B-VI	B-VI (PT)	J-3.2	ABBN93
F238 / F235	0.0213	0.0222	0.0217	0.0219	0.0212	0.0215
C / E		1.042	1.019	1.028	0.995	1.009

Table 9 (cont'd). Sample calculation results

	$E_{benchmark}$	B-V	B-VI	B-VI (PT)	J-3.2	ABBN93
F239 / F235	0.944	0.960	0.940	0.943	0.944	0.946
C / E		1.017	0.996	0.999	1.000	1.002

The perfect agreement between the all calculation and benchmark results is observed for ^{239}Pu-to-^{235}U fission rate ratio and C/E values not exceed the experimental error. The difference for ^{238}U-to-^{235}U fission rate ratio rather higher, but only ENDF/B-V result exceeds experimental error in two times.

4.3 Fission Rate Distributions

This item is the most interesting (of course, after criticality) because all previous reports and papers, for example /7, 8, 10/, demonstrate the very big discrepancies between calculation and experimental values for stainless steel region of the BFS-62-3A assembly obtained by traditional deterministic methods. What will be a situation with continuous energy or multi-group Monte Carlo calculations? So, fission rate distributions were included in present benchmark specification expressly to answer on one simple question: are the modern initial neutron data files good or not to resolve this problem?

The primary calculation model was slightly modified such way to pick out special cylindrical subzones inside steel reflector where fission rates will be computed. Each ring had 2.5 cm thickness and 8 cm height on the core midplane level. The total number of such calculation subzones is 14. This calculation model is included in Appendix also. MCNP tallies also were used to calculate ^{235}U, ^{238}U and ^{239}Pu fission rates in these regions. Then the obtained values were divided by central point as well as experimental results. The calculations used 20,000 neutron histories per generation and 5,000 active generations after skipping 10. The statistical errors are very negligible and not exceed 0.5%. The following Figures 4~6 present calculation and experimental fission rate distributions along stainless steel reflector.

Looking at these figures easily to mark that general picture is the same like in previous works mentioned above, i.e. there is big overestimation for ^{235}U and ^{239}Pu fission rates (approx. 10~20%); and underestimation for ^{238}U fission rate is on the same level. The minimum level of discrepancies has ENDF/B-V data and the maximum one - ENDF/B-VI data. However, it is known that ENDF/B-V data library for MCNP calculations has the artificially corrected file of iron /11/. This correction was made by Los-Alamos Laboratory to describe the criticality of the steel (iron) reflected small cores much better. Nevertheless, even these cross sections not allow to describe fission rate distributions better than 10%. Cross sections from JENDL-3.2 and ABBN-93 have practically the same values and depict the distributions slightly better than ENDF/B-VI.

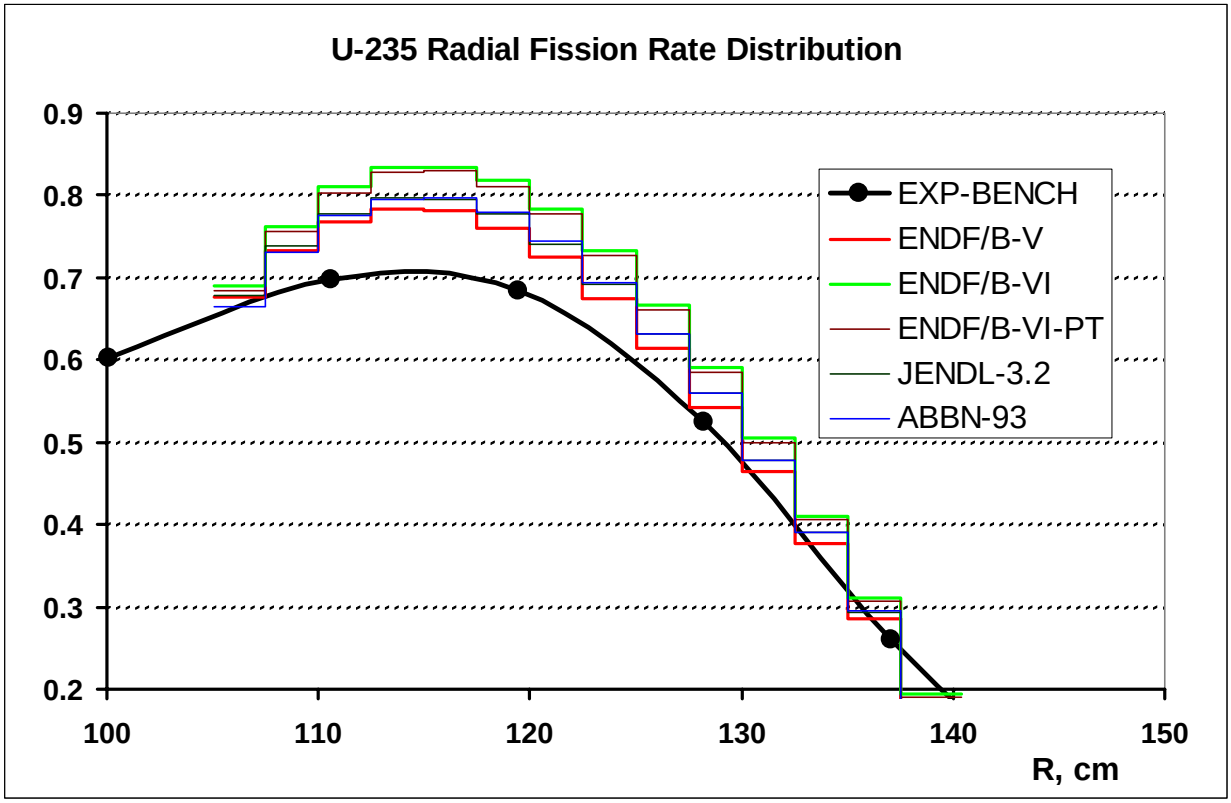

Fig. 4. ^{235}U fission rate distribution

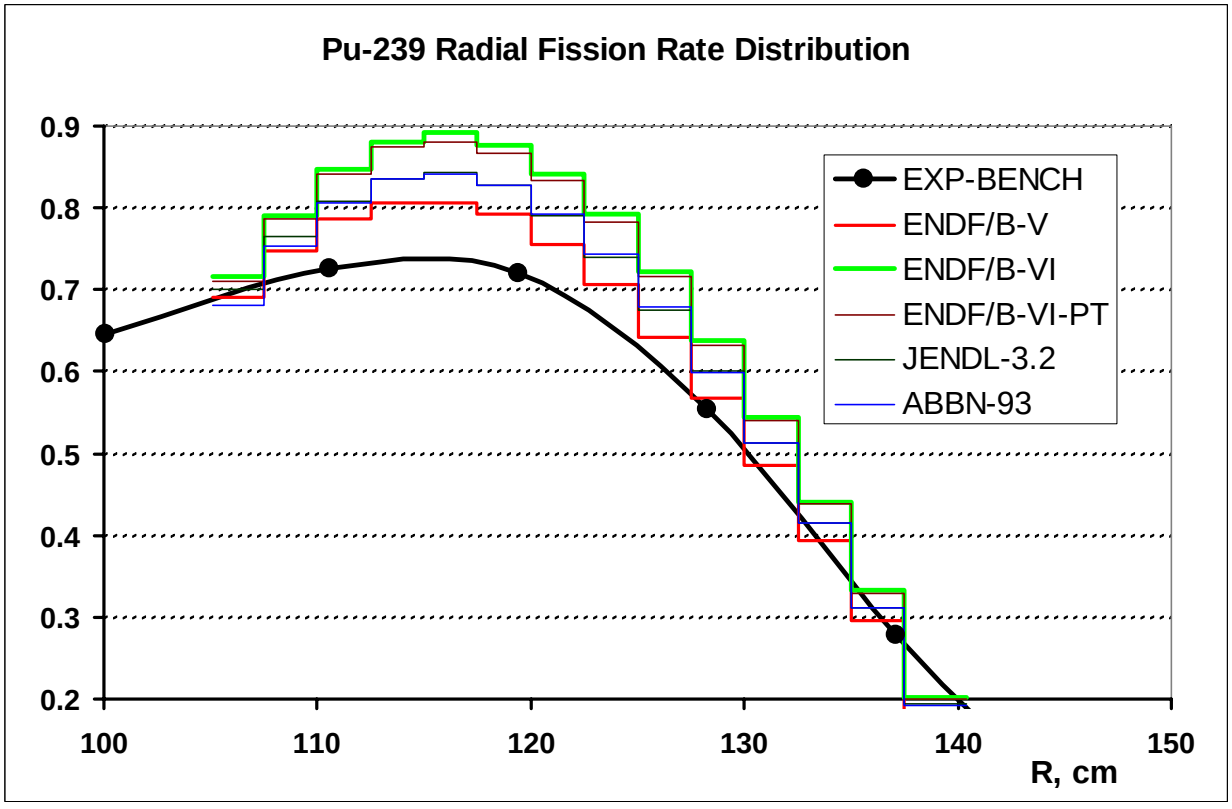

Fig. 5. ^{239}Pu fission rate distribution

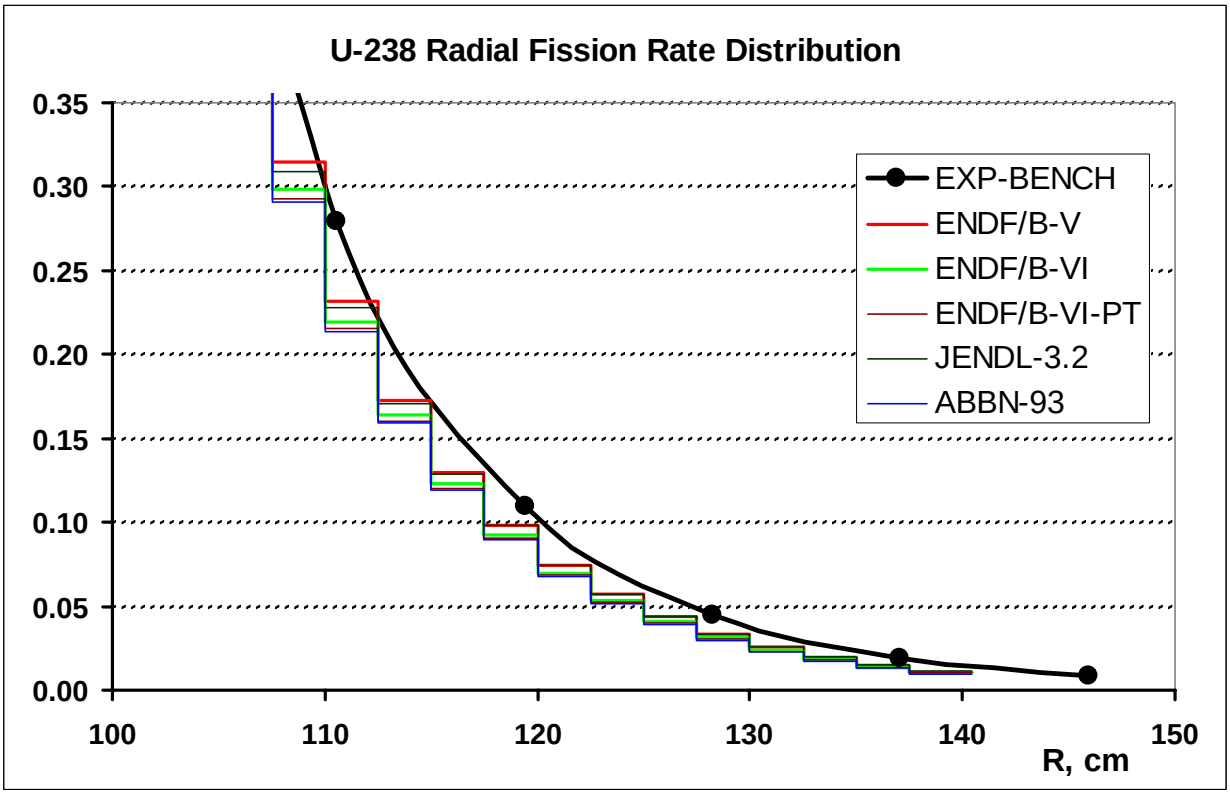

Fig. 6. ^{238}U fission rate distribution

What can be a reason of these discrepancies? Since the fission rate is the product of the total flux and one-group cross section, let's consider separately flux and cross sections behaviors along steel reflector and in core center, also. To understand the scale of discrepancies, I'm suggesting to examine ratios of these values, divided, say, by ABBN-93 data. The results are presented in Table 10 and on Figures 7~10 below.

Table 10. Flux and fission cross sections ratios for core center (divided by ABBN-93)

Parameter	ENDF/B-V	ENDF/B-VI	JENDL-3.2
Flux	0.958	0.998	0.990
^{235}U	0.973	0.993	1.002
^{239}Pu	0.988	0.987	1.000
^{238}U	1.004	1.000	0.986

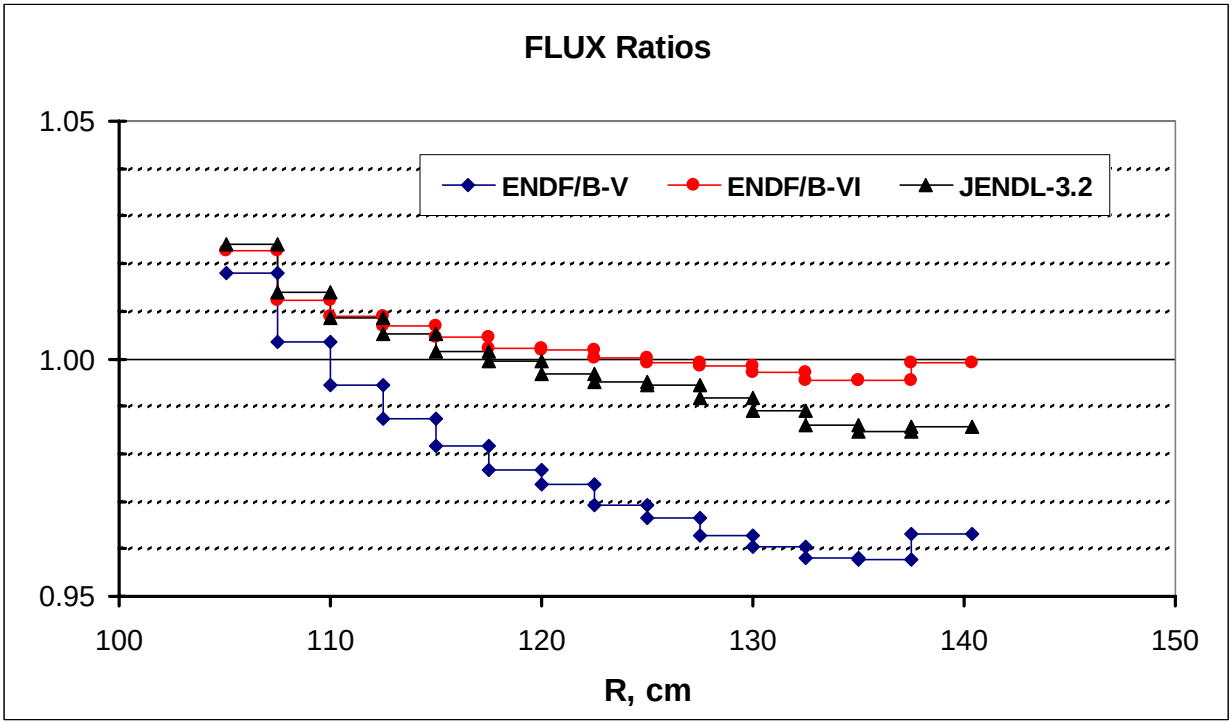

Fig. 7. Flux ratios distributions along steel reflector

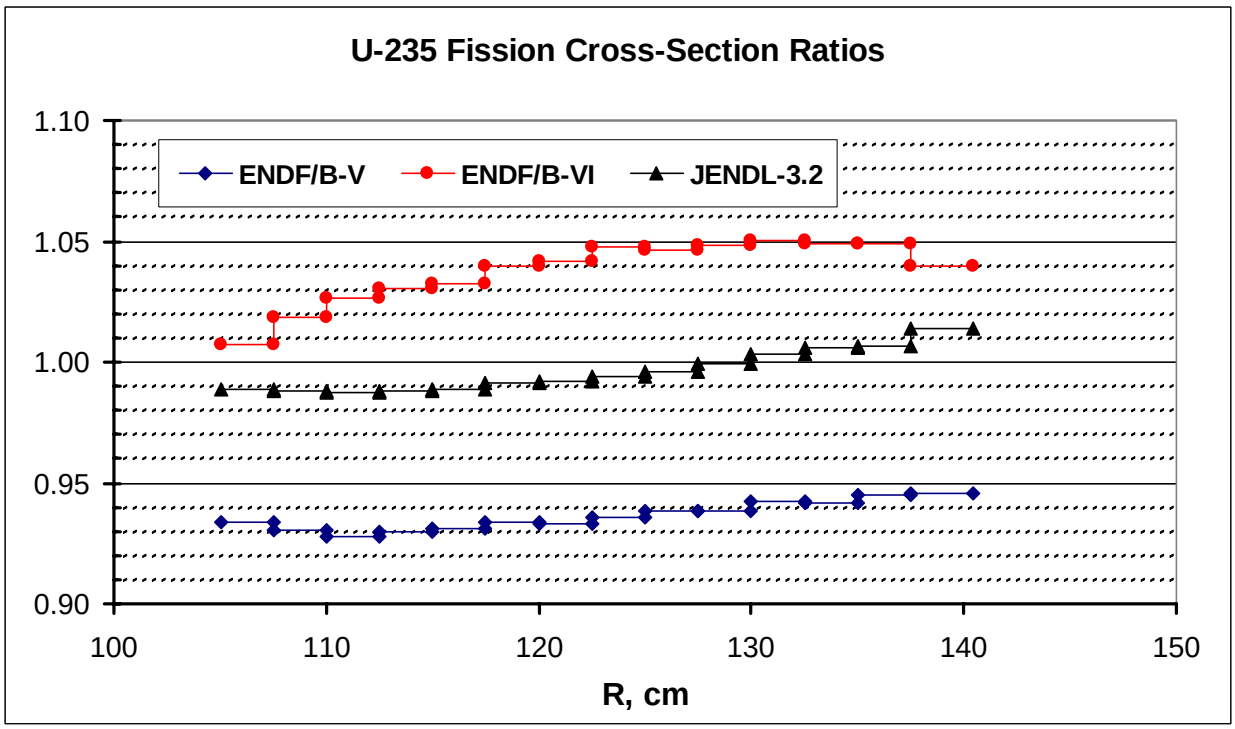

Fig. 8. ^{235}U fission cross section ratios distributions

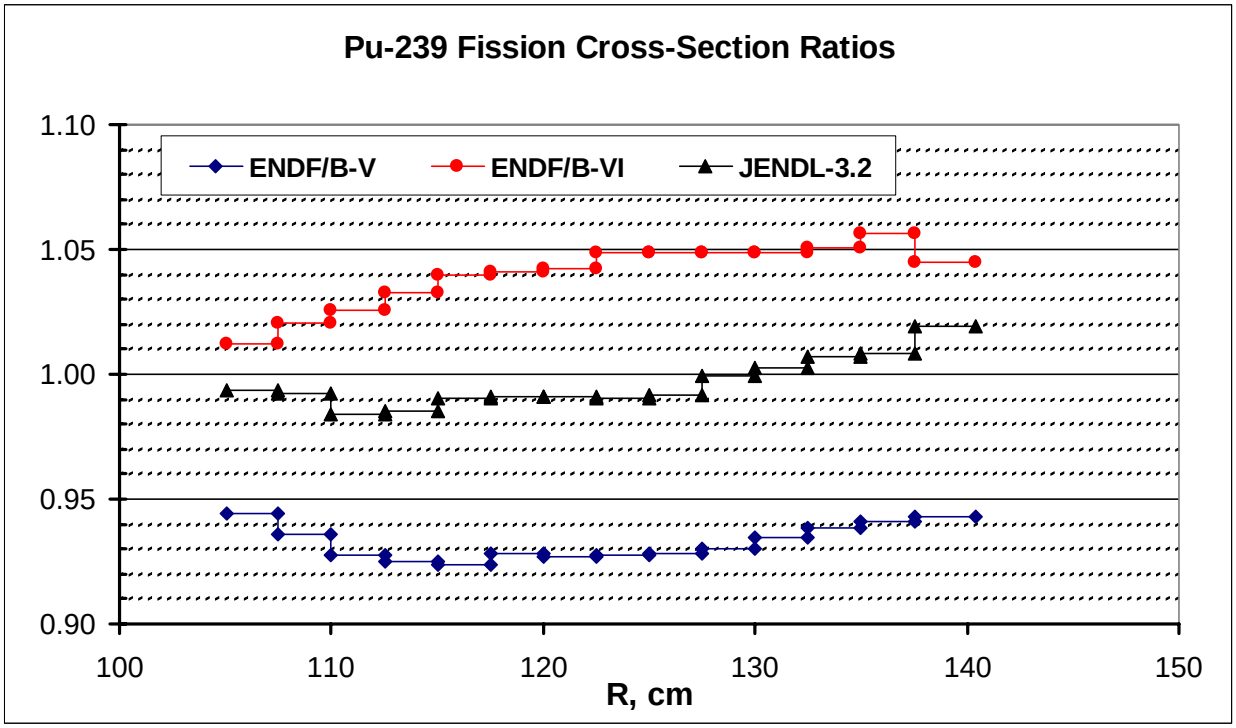

Fig. 9. ^{239}Pu fission cross section ratios distributions

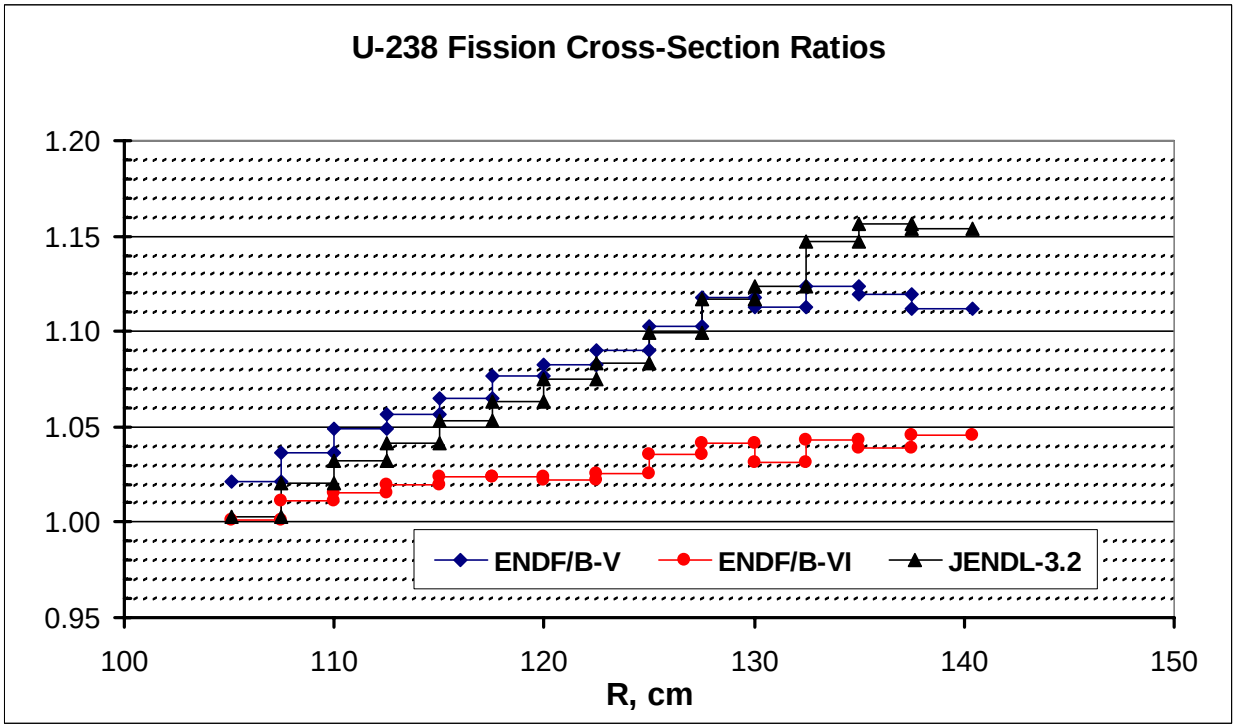

Fig. 10. ^{238}U fission cross section ratios distributions

If we consider core center parameters (Table 10), it easy to note that all values are in good or reasonable, at least, agreement with each other.

Perhaps, the flux and ^{235}U fission cross section values with ENDF/B-V data are slightly lower (3~4%) than another but these separate discrepancies give –7% in fission rate. This tendency is preserved and for steel region amounting to –10% in deep layers. The analogous dependence is observed for ^{239}Pu fission rate distribution, also. As regards ^{238}U fission rate distribution, the cross section tendency has a reverse direction than flux one and these values partially compensate each other. The fission rate ratio (ENDF/B-V-to-ABBN-93 data) for steel region is +6±2% in average.

More modern American data (ENDF/B-VI) have perfect agreement with Russian results both for flux and for cross sections in the core center. Flux ratios are very stable inside reflector volume and maximum discrepancies (+2%) are observed only nearby core boundary. All fission cross section ratios have the similar monotonous tendencies and practically the same values exceeding ABBN-93 data on ~5% in deep layers of the steel region.

JENDL-3.2 data also have perfect agreement with ABBN-93 results both for flux and for cross sections in the core center, like ENDF/B-VI. Moreover, this excellent agreement is preserved for ^{235}U and ^{239}Pu fission cross sections inside steel region too. As regards ^{238}U fission cross section, the trend is very similar to ENDF/B-V one and difference between two neutron data achieves 15% far from core region. Taking into account that these parameters are practically the same in core center, in all probability, this fact can be explained harder spectrum, which is formed by steel components, and first of all – by iron, in deep layers of the steel region. Or, may be, ^{238}U fission cross section in JENDL-3.2 has big under threshold values, which is beginning appreciable under soft spectrum.

Of course, all modern investigated neutron data have some distinctions but on practice the fission rate distributions are described equally in general. Taking into account the fact that such global parameter like k_{eff} is predicted well enough and central spectral indices have good agreement in core center, I can propose that existing neutron files for steel components are not good. True, besides there is a probability that the reported steel passport isn't correct and additional capture presents in real composition. This problem is under investigation at IPPE now.

5. NEUTRON DATA FILES TESTING

To understand 1) what a “degree of belief” to obtained criticality results and 2) why the underestimation of this parameter with ENDF/B-V data such big, I decided to check the cross sections of major isotopes on very wide benchmark criticality collection. Conditionally these benchmarks can be divided on three classes, which are interesting as applied to our present goals:

1) So-called “small systems”, i.e. bare or reflected assemblies of Godiva or Flattop class;
2) Reactor class benchmarks;
3) Special class of the fast critical assemblies with steel reflector.

Typical samples of the neutron spectrums for these benchmarks are shown on Fig. 11.

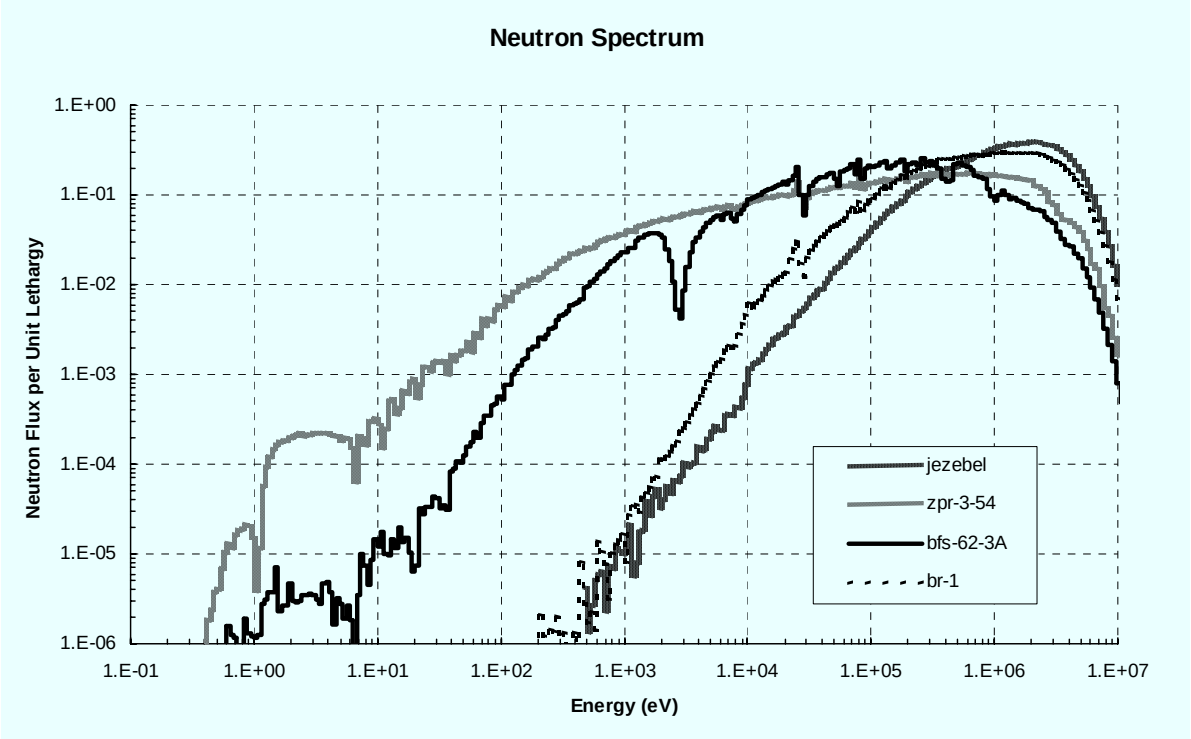

Fig. 11 Benchmark neutron spectrums

5.1 Small Systems

As a rule, these assemblies are characterized by one (or maximum – two) dominating isotope inside core or reflector. This isotope itself forms the neutron spectrum. The assemblies are characterized by high neutron leakage also. I expressly selected the assemblies with different enrichments to analyze the degree of influence on criticality of the different isotopes.

All calculation models were derived from International Handbook /12-14/. It is very easily to find them by name or by identification number. The main characteristics of these benchmarks are given in Table 11.

Table 11. Short description of the small benchmark systems

Type	Name	Core (Enrichment, %w.)	R (core) cm	Reflector	ΔR (reflector) cm
BARE	Jezebel	Pu-239 (95%)	6.38493	-	-
	Jezebel-Pu	Pu-240 (20%)	6.6595	-	-
	Godiva	U-235 (94%)	8.7407	-	-
	IMF-003	U-235 (36%)	15.324	-	-
	SCHERZO-5.56	U-235 (5.56%,a.)	Infinity	-	-
REFLECTED	Flattop-25	U-235 (93%)	6.1156	U nat.	18.0086
	Flattop-Pu	Pu-239 (95%)	4.5332	U nat.	19.6088
	IMF-002	U-235 (16%)	R= 19.05 H= 31.951	U nat.	R & H ~7.6
	Big-ten	U-235 (10%)	R= 26.67 H= 57.6338	U dep.	R= 15.24 H= 19.4431

The calculations used 5,000 neutron histories per generation and 1,000 active generations after skipping 10. The statistical errors are very negligible and not exceed 0.03% in k_{eff}. Comparison C/E values obtained with different neutron data is presented on Fig. 12.

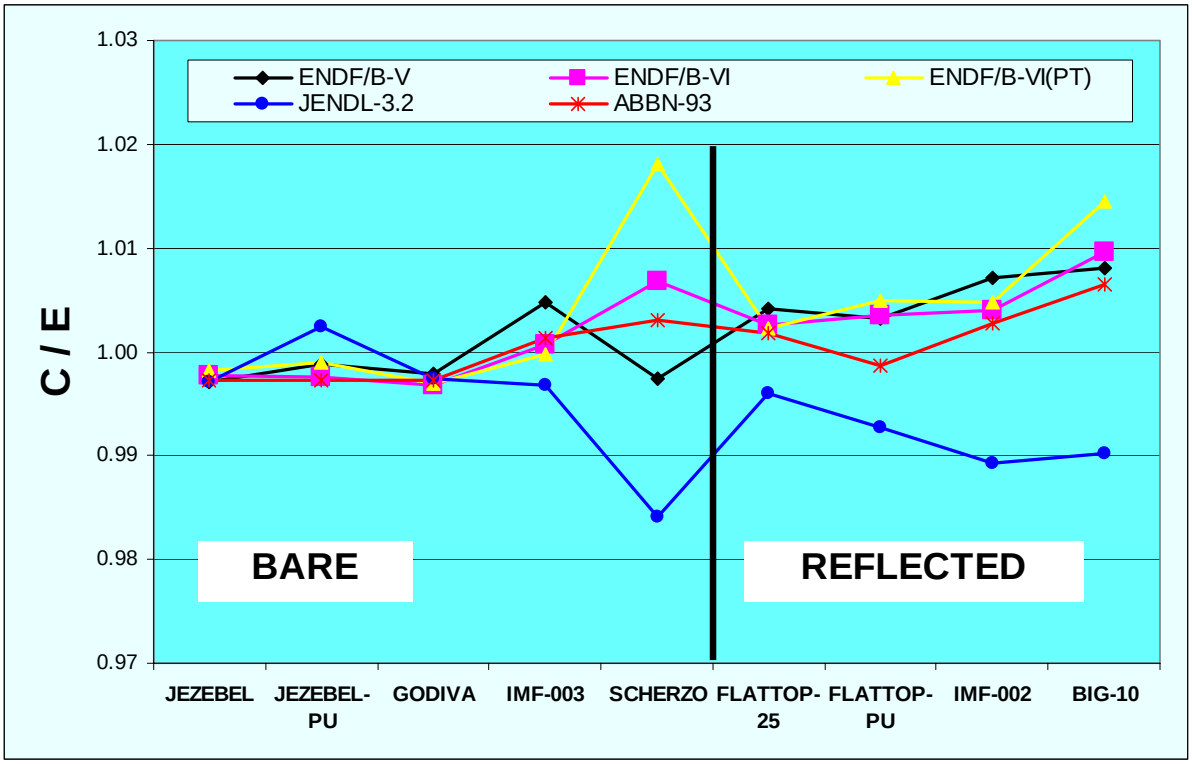

Fig. 12. C/E values for small systems

As you can see, all neutron libraries describe the main bare experiments well enough. However, as in proportion as amount of ^{238}U is increased in the core the discrepancy between calculation results are raised too and the maximum effect is observed for infinity medium SCHERZO-5.56. The lowest value has JENDL-3.2 (-1.6%) and the highest – ENDF/B-VI-PT (+1.8%) for this benchmark. It seems to me, that Japanese ^{238}U file has very low threshold of the unresolved resonance region and as a result – very many captures on this isotope. The very big difference between two ENDF/B-VI libraries allows to propose that the probability tables or, may be, the evaluated file are not very good for this nuclide. It should be mentioned, also, that there is big discrepancy between Jezebel and Jezebel-Pu results for JENDL-3.2 (0.5%), while the results obtained with the rest data are the same. Most likely, ^{240}Pu file has overestimated fission cross section in this library.

As regards the reflected systems, there are two different trends for calculation results – underestimation by JENDL-3.2 (-0.5-1.0%) and overestimation up to +1.5% by the rest data.

ABBN-93 data describe all configurations better and have the lowest discrepancies with evaluated experimental values.

5.2 Reactor Class Benchmarks

These assemblies were constructed as a different Liquid Metal Fast Breeder Reactor (LMFBR) designs with uranium or MOX fuel. That have very big core volumes with intermediate enrichment (10~30%) and neutron spectrum are formed by isotope mixture. The leakage component is too small for these systems – not more than 1~2%. The main characteristics of these benchmarks are given in Table 12.

Table 12. Short description of the reactor benchmark systems

Name	Core	Reflector
ZPR-6-6A	UO_2	U met.
ZPR-6-7	MOX	U met.
ZPPR-2	MOX	UO_2
ZPPR-9	MOX	UO_2
BFS-62-3A	UO_2+ MOX	Steel

All these models are simplified two-dimensional R-Z ones. Calculation models for ZPR-6-6A, ZPR-6-7 and ZPPR-2 were adapted for MCNP code from /15/. Heterogeneous correction factors, estimated by evaluators, were included in benchmark k_{eff}. Evaluation of benchmark k_{eff} for ZPPR-9 was made using a pair of multi-group Monte Carlo calculations with ABBN-93 data. First, ZPPR-9 was modeled in full detail – every plate, drawer, matrix tube, and air gap was modeled explicitly /16/. The simplified model was taken from /17/. This simple model is the criticality-safety benchmark model. The difference in k_{eff} values from the two models was used to adjust the measured excess reactivity of ZPPR-9, yielding a result for the benchmark model. The final benchmark k_{eff} for these assemblies are given below in Table 13.

Table 13. Benchmark k_{eff} for simplified models

Name	R-Z Benchmark-Model k_{eff}
ZPR-6-6A	0.9927 a)
ZPR-6-7	0.9834 a)
ZPPR-2	0.9825 a)
ZPPR-9	0.99049 b)
BFS-62-3A	0.99025 b)

a) Taken from evaluations

b) Calculated by author

The calculations used 1,000 neutron histories per generation and 2,000 active generations after skipping 10. The statistical errors not exceed 0.04% in k_{eff}. Comparison C/E values obtained with different neutron data is presented on Fig. 13.

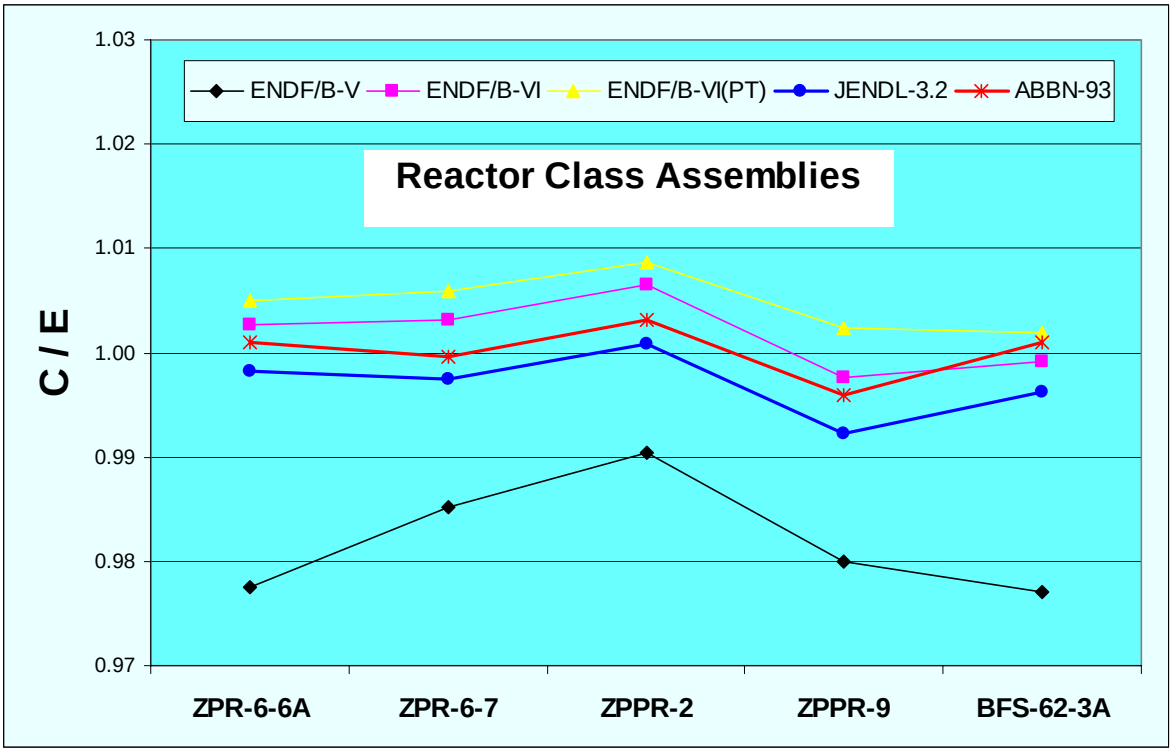

Fig. 13. C/E values for reactor class benchmarks

Analyzing of the obtained results, it is clear that supposition about uselessness ENDF/B-V data for calculation of the fast reactor system (mentioned in Section 3.1) is fully true. It may be explained that this library was created for criticality safety request, first of all, and can describe the systems with very hard or very soft spectrums.

Another libraries have the difference between each other from 0.6% to 1%, which can be assumed as a realistic evaluation of the calculation accuracy. It should be noted; ENDF/B-VI-PT data have stable overestimated results and the mean value is +0.5%. From the other hand, JENDL-3.2 data underestimate criticalities and mean value is –0.3%. ENDF/B-VI and ABBN-93 data describe all configurations slightly better and have the lowest discrepancies with evaluated benchmark k_{eff}.

5.3 Steel-Reflected Benchmarks

A few special benchmarks were investigated to estimate the steel (iron) reflector efficiency. As a rule, these assemblies were constructed together with uranium-reflected ones to estimate steel reflector efficiency. These two pairs of the assemblies have very different core neutron spectrums (see Fig. 11).

BR-1 calculation models were derived from International Handbook /12/; the rest models were adapted to MCNP code from another source /18/. Heterogeneous correction factors, estimated by evaluators /19/, were included in benchmark k_{eff}. The main characteristics and the final benchmark k_{eff} for these assemblies are given below in Table 14.

Table 14. Short description and benchmark k_{eff} for the steel-reflected systems

Name	Core	Reflector	R-Z Benchmark-Model k_{eff}
BR-1	Pu	U met.	1.0009
BR-1	Pu	FE	1.0041
ZPR-3-53	Pu+C	U met.	0.977
ZPR-3-54	Pu+C	FE	0.977

Comparison C/E values obtained with different neutron data is presented on Fig. 14.

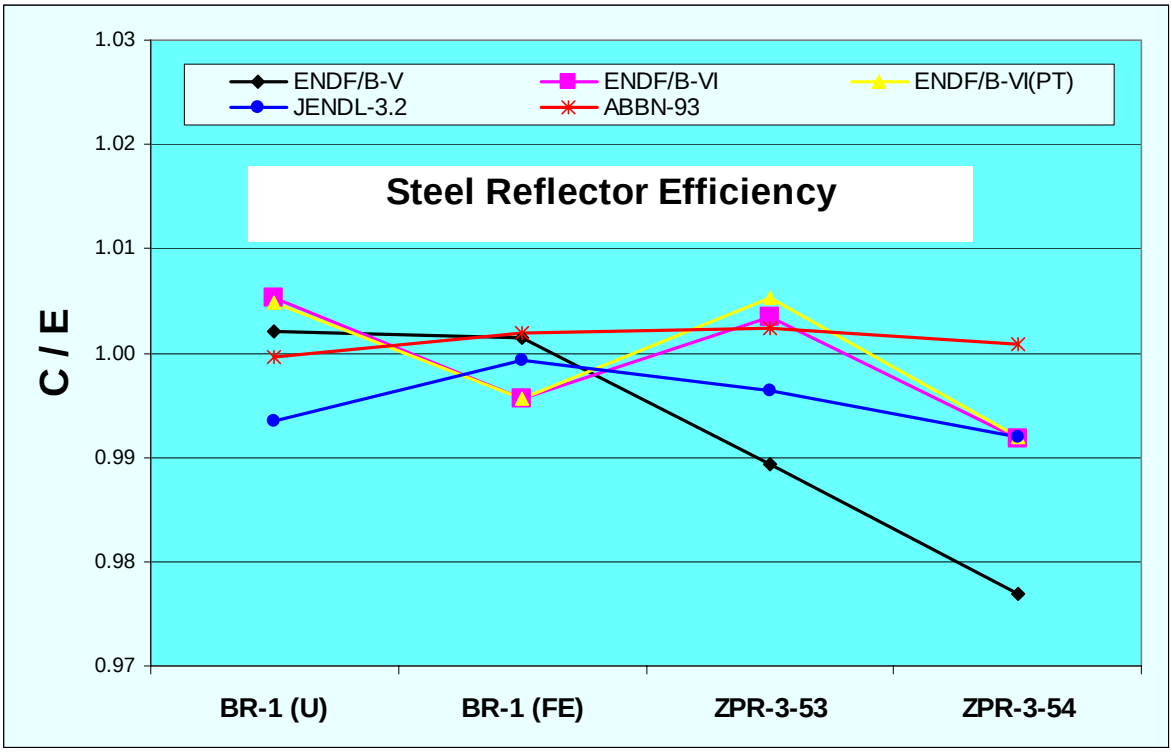

Fig. 14. C/E values for uranium-steel-reflected systems

ABBN-93 data describe and criticalities and steel reflector efficiency in best way - discrepancies for both not exceed 0.2%.

ENDF/B-V data results have the same tendencies as considered above, i.e. there is good agreement with the experiments for hard spectrum systems (BR-1) and – very big difference for softer spectrum ones.

ENDF/B-VI data have a good agreement with the experiments for uranium-reflected assemblies but for steel-reflected ones the criticalities lay on 1% lower. These results were a little unexpected because the criticality of the BFS-62-3A benchmark was predicted very well. To all appearances, it may be connected with the fact that BR-1 and ZPR-3-54 assemblies had denser reflector, which included practically pure iron.

JENDL-3.2 data underestimate the criticalities for uranium-reflected systems like in previous Sections (-0.4-0.6%) but the transition to steel reflector is calculated much better than ENDF/B-VI data.

As a whole, the maximum-minimum difference between all data libraries (if ENDF/B-V results to exclude) is on the same level (~1%) like for the reactor class benchmarks.

6. CONCLUSION

The report describes simple calculation benchmark-model of the BFS-62-3A critical assembly and presents the experimental values transformed for this model. Benchmark characteristics for this assembly are 1) criticality; 2) central fission rate ratios (spectral indices); and 3) fission rate distributions in stainless steel reflector.

The calculation results obtained by using available modern data libraries are presented also. All results were computed by Monte Carlo method.

In addition to BFS-62-3A benchmark, other criticality benchmarks, which include small systems, fast reactor assemblies and special benchmarks with steel reflector, were investigated.

It was shown that ENDF/B-V data should not be used to calculate fast reactor systems because these data have a low threshold of the unresolved resonance region (4 keV for U238 and 300 ev for Pu239, for example). Underestimation of criticality is around 2% Δk.

As for the rest data, the difference between each other in criticality for BFS-62-3A is around 0.6% Δk. However, taking into account the results obtained for others fast reactor benchmarks (and steel-reflected also), it may conclude that the difference in criticality calculation results can achieve 1% Δk. This value is in a good agreement with cross section uncertainty evaluated for BN-600 hybrid core ($\pm$0.6%Δk) /5/. As a rule, the maximum values have ENDF/B-VI data and the minimum ones – JENDL-3.2 data.

Central fission rate ratios are calculated by all data libraries very well and discrepancies with experimental values do not exceed the experimental errors.

It should be noted that Monte Carlo calculations with continuous energy cross sections cannot remove considerable inconsistency between the calculated and measurement values (15~20%), which was found for the fission rate distribution in the stainless steel reflector region by traditional deterministic methods. From my point of view, the further investigations connected with improvement of nuclear data libraries for structural elements will be useful to resolve this problem.

Unfortunately, I did not have possibility to use the newest JENDL-3.3 and JEFF-3.0 data libraries in my investigations, but I'm sure that this work will be performed in nearest future. I hope, that JENDL-3.3 library will has probability tables not only for the MVP code (like JENDL-3.2) but for the MCNP code also.

It is supposed that those results can be effectively utilized for future investigation on analysis accuracy evaluation of the BN-600 full MOX core, which will be the next step of the existing reactor state transformation after hybrid core.

7. ACKNOWLEDGEMENTS

The author is very grateful to Mr. Taira Hazama for the help in creating working version of the MCNP-4C code on workstation under LINUX and in installation MCNP-4B with JENDL-3.2 data library on my computer.

The author is very thankful to Mr. Akira Shono for the fruitful discussions and helpful comments.

REFERENCES

1. V. Dvuchsherstnov, et al., “Experimental and Calculation Studies Performed on BFS-62-3 Series”, Preprint IPPE, 2853 (2000), (in Russian).

2. I. P. Matveenko et al., “Intermediate Report #1”, JNC-IPPE Agreement on Experimental Investigation of Excess Weapon Pu Disposition in BN-600 Reactor using BFS-2 Facility, JNC ZY9200 2000-001 (2000).

3. International Handbook of Evaluated Criticality Safety Benchmark Experiments, NEA/NSC/DOC(95)03, NEA OECD (2001).

4. T. Ivanova, “Neutron Data Error Covariance Matrixes Used for Estimation of Uncertainties of Calculation Prediction of Integral Parameters for BN-600 Hybrid Core”, International Working Group Meeting on Experimental Investigation of Excess Weapons Pu Disposition in BN-600 Reactor Using BFS-2 Facility, Obninsk, Russia, September 2-5 (2002).

5. Y. Khomyakov, “BN-600 Hybrid Core Uncertainty Evaluation”, International Working Group Meeting on Experimental Investigation of Excess Weapons Pu Disposition in BN-600 Reactor Using BFS-2 Facility, Obninsk, Russia, September 2-5 (2002).

6. A. Kochetkov, I. Matveenko, V. Matveev, A. Tsiboulia, A. Shono, T. Hazama, M. Ishikawa, “BN-600 Hybrid Core Mock-Up at BFS-2 Critical Facility”, PHYSOR 2002, Seoul, Korea, October 7-10 (2002).

7. M. Semenov, Experimental Analysis Results on BFS-62-3A Using IPPE Standard System”, JNC TN9400 2002-037 (2002).

8. A. Shono, K. Sugino, T. Hazama, M. Ishikawa, Y. Khomyakov, M. Semenov, G. Manturov, “Experimental Analysis Results on BN-600 Mock-up Core Characteristics at the BFS-2 Critical Facility”, PHYSOR 2002, Seoul, Korea, October 7-10 (2002).

9. F. Maekawa, K. Sakurai, K. Kosako, E. Kume, N. Kawasaki, Y. Nomura, Y. Naito, “Development of Automatic Editing System for MCNP Library AUTONJ”, JAERI-Data/Code 99-048 (1999).

10. T. Hazama, A. Shono, T. Iwai, W. Sato, “Analyses on the BFS Critical Experiments: an Analysis on the BFS-62-3A and 62-4 Cores”, JNC TN9400 2002-036 (2002).

11. G. Manturov, “Emphasizing to the Steel Reflector Problem”, International Working Group Meeting on Experimental Investigation of Excess Weapons Pu Disposition in BN-600 Reactor Using BFS-2 Facility, Obninsk, Russia, September 2-5 (2002).

12. International Handbook of Evaluated Criticality Safety Benchmark Experiments, NEA/NSC/DOC(95)03/I, NEA OECD (2001).

13. International Handbook of Evaluated Criticality Safety Benchmark Experiments, NEA/NSC/DOC(95)03/II, NEA OECD (2001).

14. International Handbook of Evaluated Criticality Safety Benchmark Experiments, NEA/NSC/DOC(95)03/III, NEA OECD (2001).

15. ENDF-202, CSEWG Benchmark Specifications, BNL 19302 (1978).

16. M. Ishikawa et al., “Development of a Standard Data Base for FBR Core Nuclear Design (VIII)”, PNC TN9410 97-099 (1997).

17. T. Iwai, K. Sugino, M. Ishikawa, “ Development of the ZPPR-9 Core Benchmark Problem”, PNC TN9410 98-079 (1998).

18. R. E. Kaiser, et al., “Measurements of Neutron Spectrum and Spectral Indices in ZPR-3 Assemblies 53 and 54”, ANL, ZPR-TM-16 (1970).

19. R. W. Hardie et al., “An Analysis of Selected Fast Critical Assemblies Using ENDF/B-IV Neutron Cross Sections”, NSE, v. 57(3), p.222 (1975).

Appendix

MCNP ENDF/B-VI Input Listing (Benchmark Criticality Model)

```
BFS-62-3A Benchmark Model
1   1 4.927452E-02      -1 102 -103 imp:n=1
2   1 4.927452E-02   1  -2 102 -103 imp:n=1
3   1 4.927452E-02   3  -4 102 -103 imp:n=1
4   1 4.927452E-02   5  -6 102 -103 imp:n=1
5   2 4.971844E-02   6  -7 102 -103 imp:n=1
6   3 4.949116E-02   8  -9 102 -103 imp:n=1
7   4 5.098051E-02   9 -10 102 -103 imp:n=1
8   5 5.101812E-02  10 -11 102 -103 imp:n=1
9   6 5.318676E-02  11 -12 100 -107 imp:n=1
10  7 6.302118E-02  12 -13 100 -107 imp:n=1
11  8 5.373813E-02  13 -14 100 -107 imp:n=1
12  9 4.947017E-02      -2 101 -102 imp:n=1
13  9 4.947017E-02   3  -4 101 -102 imp:n=1
14  9 4.947017E-02   5  -7 101 -102 imp:n=1
15  9 4.947017E-02   8 -11 101 -102 imp:n=1
16 10 4.938500E-02      -2 103 -105 imp:n=1
17 10 4.938500E-02   3  -4 103 -105 imp:n=1
18 10 4.938500E-02   5  -7 103 -105 imp:n=1
19 10 4.938500E-02   8 -11 103 -105 imp:n=1
20 11 5.429148E-02      -2 105 -107 imp:n=1
21 11 5.429148E-02   3  -4 105 -107 imp:n=1
22 11 5.429148E-02   5  -7 105 -107 imp:n=1
23 11 5.429148E-02   8 -11 105 -107 imp:n=1
24 12 4.715875E-02   2  -3 101 -104 imp:n=1
25 12 4.715875E-02   4  -5 101 -104 imp:n=1
26 12 4.715875E-02   7  -8 101 -104 imp:n=1
27 13 5.392302E-02   2  -3 104 -106 imp:n=1
28 13 5.392302E-02   7  -8 104 -106 imp:n=1
29 14 2.029320E-02     -11 100 -101 imp:n=1
30 15 8.480486E-02   4  -5 104 -106 imp:n=1
31 16 1.001539E-02   2  -3 106 -107 imp:n=1
32 16 1.001539E-02   4  -5 106 -107 imp:n=1
33 16 1.001539E-02   7  -8 106 -107 imp:n=1
34  0              14:-100:107 imp:n=0

1   cz   5.3554
2   cz  37.1253
3   cz  39.3747
4   cz  47.6985
5   cz  49.4695
6   cz  63.3091
7   cz  70.6931
8   cz  73.0868
9   cz  83.2672
10  cz  96.6569
11  cz 105.0802
12  cz 140.414
13  cz 149.247
14  cz 169.913
100 pz   0.0
101 pz  25.0
102 pz  60.4
103 pz 164.21
104 pz 170.579
105 pz 193.6
106 pz 220.289
107 pz 233.46
```

```
m1 1001.60c 1.4530E-05 11023.60c 6.5728E-03  6000.60c 3.0251E-04 &
  13027.60c 5.0165E-03 22000.60c 1.2084E-04 24050.60c 1.3791E-04 &
  24052.60c 2.6595E-03 24053.60c 3.0157E-04 24054.60c 7.5067E-05 &
  25055.60c 2.5034E-04 26054.60c 6.7276E-04 26056.60c 1.0561E-02 &
  26057.60c 2.4390E-04 26058.60c 3.2458E-05 28058.60c 1.0103E-03 &
  28060.60c 3.8918E-04 28061.60c 1.6919E-05 28062.60c 5.3932E-05 &
  28064.60c 1.3743E-05 92235.60c 1.0642E-03 92238.60c 6.5656E-03 &
   8016.60c 1.3199E-02
m2 1001.60c 1.5820E-05 11023.60c 6.5728E-03  6000.60c 3.0195E-04 &
  13027.60c 5.0196E-03 22000.60c 1.1997E-04 24050.60c 1.3690E-04 &
  24052.60c 2.6399E-03 24053.60c 2.9935E-04 24054.60c 7.4514E-05 &
  25055.60c 2.4850E-04 26054.60c 6.7025E-04 26056.60c 1.0521E-02 &
  26057.60c 2.4299E-04 26058.60c 3.2337E-05 28058.60c 1.0029E-03 &
  28060.60c 3.8632E-04 28061.60c 1.6794E-05 28062.60c 5.3536E-05 &
  28064.60c 1.3642E-05 92235.60c 1.2222E-03 92238.60c 6.8447E-03 &
   8016.60c 1.3282E-02
m3 1001.60c 5.0247E-06 11023.60c 6.2598E-03  6000.60c 4.0190E-04 &
  13027.60c 2.4161E-03 22000.60c 1.3688E-04 25055.60c 2.8976E-04 &
  92235.60c 1.4786E-03 92238.60c 6.7585E-03  8016.60c 1.3240E-02 &
  24050.60c 1.5794E-04 24052.60c 3.0456E-03 24053.60c 3.4535E-04 &
  24054.60c 8.5965E-05 26054.60c 7.6967E-04 26056.60c 1.2082E-02 &
  26057.60c 2.7903E-04 26058.60c 3.7134E-05 28058.60c 1.1585E-03 &
  28060.60c 4.4624E-04 28061.60c 1.9399E-05 28062.60c 6.1840E-05 &
  28064.60c 1.5758E-05
m4 1001.60c 5.4267E-06 11023.60c 5.6338E-03  6000.60c 4.2824E-04 &
  13027.60c 2.5889E-03 22000.60c 1.3838E-04 25055.60c 2.9177E-04 &
  92235.60c 2.9720E-05 92238.60c 7.1145E-03  8016.60c 1.4299E-02 &
  94239.60c 1.4501E-03 94240.60c 7.0234E-05 94241.60c 8.0423E-07 &
  95241.60c 2.9419E-06 31000.60c 8.7691E-05 24050.60c 1.6073E-04 &
  24052.60c 3.0996E-03 24053.60c 3.5147E-04 24054.60c 8.7488E-05 &
  26054.60c 7.8381E-04 26056.60c 1.2304E-02 26057.60c 2.8416E-04 &
  26058.60c 3.7816E-05 28058.60c 1.1775E-03 28060.60c 4.5358E-04 &
  28061.60c 1.9719E-05 28062.60c 6.2857E-05 28064.60c 1.6017E-05
m5 1001.60c 1.0623E-05 11023.60c 5.6338E-03  6000.60c 3.6591E-04 &
  13027.60c 4.0036E-03 22000.60c 1.3132E-04 25055.60c 2.7457E-04 &
  92235.60c 1.8646E-03 92238.60c 7.0132E-03  8016.60c 1.4148E-02 &
  24050.60c 1.4974E-04 24052.60c 2.8875E-03 24053.60c 3.2742E-04 &
  24054.60c 8.1503E-05 26054.60c 7.3138E-04 26056.60c 1.1481E-02 &
  26057.60c 2.6515E-04 26058.60c 3.5287E-05 28058.60c 1.0983E-03 &
  28060.60c 4.2306E-04 28061.60c 1.8392E-05 28062.60c 5.8627E-05 &
  28064.60c 1.4939E-05
m6 6000.60c 2.4180E-04 13027.60c 9.1493E-04 22000.60c 3.7607E-04 &
  25055.60c 7.9296E-04 24050.60c 4.3685E-04 24052.60c 8.4241E-03 &
  24053.60c 9.5523E-04 24054.60c 2.3778E-04 26054.60c 2.1104E-03 &
  26056.60c 3.3129E-02 26057.60c 7.6509E-04 26058.60c 1.0182E-04 &
  28058.60c 3.2003E-03 28060.60c 1.2327E-03 28061.60c 5.3591E-05 &
  28062.60c 1.7083E-04 28064.60c 4.3531E-05
m7 6000.60c 1.1414E-02 13027.60c 1.0477E-04 22000.60c 4.3066E-05 &
  25055.60c 9.0806E-05  5010.60c 9.0632E-03  5011.60c 3.6481E-02 &
  24050.60c 5.0024E-05 24052.60c 9.6466E-04 24053.60c 1.0939E-04 &
  24054.60c 2.7228E-05 26054.60c 2.4167E-04 26056.60c 3.7938E-03 &
  26057.60c 8.7614E-05 26058.60c 1.1660E-05 28058.60c 3.6649E-04 &
  28060.60c 1.4117E-04 28061.60c 6.1371E-06 28062.60c 1.9563E-05 &
  28064.60c 4.9850E-06
m8 1001.60c 1.0700E-05  6000.60c 6.9662E-04 13027.60c 4.5454E-03 &
  22000.60c 4.3066E-05 25055.60c 9.0806E-05 92235.60c 5.8599E-05 &
  92238.60c 1.4028E-02  8016.60c 2.8194E-02 24050.60c 5.0024E-05 &
  24052.60c 9.6466E-04 24053.60c 1.0939E-04 24054.60c 2.7228E-05 &
  26054.60c 2.5609E-04 26056.60c 4.0200E-03 26057.60c 9.2840E-05 &
  26058.60c 1.2355E-05 28058.60c 3.6649E-04 28060.60c 1.4117E-04 &
  28061.60c 6.1371E-06 28062.60c 1.9563E-05 28064.60c 4.9850E-06
```

```
m9 1001.60c 2.4569E-04 11023.60c 5.5007E-03  6000.60c 4.9780E-04 &
  13027.60c 3.1458E-03 22000.60c 8.6518E-05 25055.60c 1.8243E-04 &
  92235.60c 3.8735E-05 92238.60c 9.2725E-03  8016.60c 1.8636E-02 &
  24050.60c 1.0050E-04 24052.60c 1.9380E-03 24053.60c 2.1976E-04 &
  24054.60c 5.4702E-05 26054.60c 4.9504E-04 26056.60c 7.7711E-03 &
  26057.60c 1.7947E-04 26058.60c 2.3884E-05 28058.60c 7.3625E-04 &
  28060.60c 2.8360E-04 28061.60c 1.2329E-05 28062.60c 3.9302E-05 &
  28064.60c 1.0015E-05
m10 1001.60c 7.0993E-06 11023.60c 5.5276E-03  6000.60c 4.9949E-04 &
  13027.60c 3.1570E-03 22000.60c 8.6577E-05 25055.60c 1.8255E-04 &
  92235.60c 3.8880E-05 92238.60c 9.3072E-03  8016.60c 1.8706E-02 &
  24050.60c 1.0057E-04 24052.60c 1.9394E-03 24053.60c 2.1991E-04 &
  24054.60c 5.4740E-05 26054.60c 4.9541E-04 26056.60c 7.7769E-03 &
  26057.60c 1.7960E-04 26058.60c 2.3902E-05 28058.60c 7.3673E-04 &
  28060.60c 2.8379E-04 28061.60c 1.2337E-05 28062.60c 3.9327E-05 &
  28064.60c 1.0021E-05
m11 1001.60c 3.5320E-04 11023.60c 8.1420E-03  6000.60c 2.0820E-04 &
  13027.60c 7.8779E-04 22000.60c 3.2381E-04 25055.60c 6.8278E-04 &
  24050.60c 3.7614E-04 24052.60c 7.2535E-03 24053.60c 8.2249E-04 &
  24054.60c 2.0474E-04 26054.60c 1.8172E-03 26056.60c 2.8525E-02 &
  26057.60c 6.5878E-04 26058.60c 8.7671E-05 28058.60c 2.7556E-03 &
  28060.60c 1.0615E-03 28061.60c 4.6145E-05 28062.60c 1.4710E-04 &
  28064.60c 3.7483E-05
m12 11023.60c 1.0936E-02  6000.60c 1.6468E-04 13027.60c 6.2311E-04 &
  22000.60c 2.5612E-04 25055.60c 5.4004E-04 24050.60c 2.9751E-04 &
  24052.60c 5.7372E-03 24053.60c 6.5055E-04 24054.60c 1.6194E-04 &
  26054.60c 1.4373E-03 26056.60c 2.2562E-02 26057.60c 5.2106E-04 &
  26058.60c 6.9344E-05 28058.60c 2.1796E-03 28060.60c 8.3956E-04 &
  28061.60c 3.6498E-05 28062.60c 1.1635E-04 28064.60c 2.9647E-05
m13 11023.60c 9.8043E-03  6000.60c 6.0934E-03 13027.60c 2.4029E-04 &
  22000.60c 9.8771E-05 25055.60c 2.0826E-04  5010.60c 4.8000E-03 &
   5011.60c 1.9320E-02 24050.60c 1.1473E-04 24052.60c 2.2124E-03 &
  24053.60c 2.5087E-04 24054.60c 6.2448E-05 26054.60c 5.5427E-04 &
  26056.60c 8.7008E-03 26057.60c 2.0094E-04 26058.60c 2.6741E-05 &
  28058.60c 8.4055E-04 28060.60c 3.2378E-04 28061.60c 1.4076E-05 &
  28062.60c 4.4869E-05 28064.60c 1.1433E-05
m14 6000.60c 9.2259E-05 13027.60c 3.4909E-04 22000.60c 1.4349E-04 &
  25055.60c 3.0256E-04 24050.60c 1.6668E-04 24052.60c 3.2142E-03 &
  24053.60c 3.6447E-04 24054.60c 9.0724E-05 26054.60c 8.0521E-04 &
  26056.60c 1.2640E-02 26057.60c 2.9191E-04 26058.60c 3.8848E-05 &
  28058.60c 1.2211E-03 28060.60c 4.7036E-04 28061.60c 2.0448E-05 &
  28062.60c 6.5183E-05 28064.60c 1.6610E-05
m15 6000.60c 1.5003E-02 13027.60c 1.7229E-04 22000.60c 7.0817E-05 &
  25055.60c 1.4932E-04  5010.60c 1.1907E-02  5011.60c 4.7925E-02 &
  24050.60c 8.2260E-05 24052.60c 1.5863E-03 24053.60c 1.7987E-04 &
  24054.60c 4.4774E-05 26054.60c 3.9740E-04 26056.60c 6.2384E-03 &
  26057.60c 1.4407E-04 26058.60c 1.9173E-05 28058.60c 6.0264E-04 &
  28060.60c 2.3213E-04 28061.60c 1.0092E-05 28062.60c 3.2169E-05 &
  28064.60c 8.1972E-06
m16 6000.60c 4.5532E-05 13027.60c 1.7229E-04 22000.60c 7.0817E-05 &
  25055.60c 1.4932E-04 24050.60c 8.2260E-05 24052.60c 1.5863E-03 &
  24053.60c 1.7987E-04 24054.60c 4.4774E-05 26054.60c 3.9740E-04 &
  26056.60c 6.2384E-03 26057.60c 1.4407E-04 26058.60c 1.9173E-05 &
  28058.60c 6.0264E-04 28060.60c 2.3213E-04 28061.60c 1.0092E-05 &
  28062.60c 3.2169E-05 28064.60c 8.1972E-06
kcode 5000 1 10 20010
ksrc 0. 0. 112.305
prdmp 3j 1
print
```

MCNP ENDF/B-VI Input Listing (Reaction Rate Distribution Model)

```
BFS-62-3A Benchmark Model
1   1 4.927452E-02      -1 102 -201 imp:n=1
2   1 4.927452E-02   1  -2 102 -103 imp:n=1
3   1 4.927452E-02   3  -4 102 -103 imp:n=1
4   1 4.927452E-02   5  -6 102 -103 imp:n=1
5   2 4.971844E-02   6  -7 102 -103 imp:n=1
6   3 4.949116E-02   8  -9 102 -103 imp:n=1
7   4 5.098051E-02   9 -10 102 -103 imp:n=1
8   5 5.101812E-02  10 -11 102 -103 imp:n=1
9   6 5.318676E-02  11 -12 100 -201 imp:n=1
10  7 6.302118E-02  12 -13 100 -107 imp:n=1
11  8 5.373813E-02  13 -14 100 -107 imp:n=1
12  9 4.947017E-02      -2 101 -102 imp:n=1
13  9 4.947017E-02   3  -4 101 -102 imp:n=1
14  9 4.947017E-02   5  -7 101 -102 imp:n=1
15  9 4.947017E-02   8 -11 101 -102 imp:n=1
16 10 4.938500E-02      -2 103 -105 imp:n=1
17 10 4.938500E-02   3  -4 103 -105 imp:n=1
18 10 4.938500E-02   5  -7 103 -105 imp:n=1
19 10 4.938500E-02   8 -11 103 -105 imp:n=1
20 11 5.429148E-02      -2 105 -107 imp:n=1
21 11 5.429148E-02   3  -4 105 -107 imp:n=1
22 11 5.429148E-02   5  -7 105 -107 imp:n=1
23 11 5.429148E-02   8 -11 105 -107 imp:n=1
24 12 4.715875E-02   2  -3 101 -104 imp:n=1
25 12 4.715875E-02   4  -5 101 -104 imp:n=1
26 12 4.715875E-02   7  -8 101 -104 imp:n=1
27 13 5.392302E-02   2  -3 104 -106 imp:n=1
28 13 5.392302E-02   7  -8 104 -106 imp:n=1
29 14 2.029320E-02     -11 100 -101 imp:n=1
30 15 8.480486E-02   4  -5 104 -106 imp:n=1
31 16 1.001539E-02   2  -3 106 -107 imp:n=1
32 16 1.001539E-02   4  -5 106 -107 imp:n=1
33 16 1.001539E-02   7  -8 106 -107 imp:n=1
34  6 5.318676E-02  11 -12 202 -107 imp:n=1
35  6 5.318676E-02  11 -301 201 -202 imp:n=1
36  6 5.318676E-02 301 -302 201 -202 imp:n=1
37  6 5.318676E-02 302 -303 201 -202 imp:n=1
38  6 5.318676E-02 303 -304 201 -202 imp:n=1
39  6 5.318676E-02 304 -305 201 -202 imp:n=1
40  6 5.318676E-02 305 -306 201 -202 imp:n=1
41  6 5.318676E-02 306 -307 201 -202 imp:n=1
42  6 5.318676E-02 307 -308 201 -202 imp:n=1
43  6 5.318676E-02 308 -309 201 -202 imp:n=1
44  6 5.318676E-02 309 -310 201 -202 imp:n=1
45  6 5.318676E-02 310 -311 201 -202 imp:n=1
46  6 5.318676E-02 311 -312 201 -202 imp:n=1
47  6 5.318676E-02 312 -313 201 -202 imp:n=1
48  6 5.318676E-02 313 -12  201 -202 imp:n=1
49  1 4.927452E-02      -1  201 -202 imp:n=1
50  1 4.927452E-02      -1  202 -103 imp:n=1
51  0              14:-100:107 imp:n=0

1 cz    5.3554
2 cz   37.1253
3 cz   39.3747
4 cz   47.6985
5 cz   49.4695
```

```
6 cz   63.3091
7 cz   70.6931
8 cz   73.0868
9 cz   83.2672
10 cz  96.6569
11 cz 105.0802
12 cz 140.414
13 cz 149.247
14 cz 169.913
100 pz 0.0
101 pz 25.0
102 pz 60.4
103 pz 164.21
104 pz 170.579
105 pz 193.6
106 pz 220.289
107 pz 233.46
c central layer
201 pz 108.4
202 pz 116.21
c reflector
301 cz 107.5
302 cz 110.
303 cz 112.5
304 cz 115.
305 cz 117.5
306 cz 120.
307 cz 122.5
308 cz 125.
309 cz 127.5
310 cz 130.
311 cz 132.5
312 cz 135.
313 cz 137.5

m1 1001.60c 1.4530E-05 11023.60c 6.5728E-03  6000.60c 3.0251E-04 &
  13027.60c 5.0165E-03 22000.60c 1.2084E-04 24050.60c 1.3791E-04 &
  24052.60c 2.6595E-03 24053.60c 3.0157E-04 24054.60c 7.5067E-05 &
  25055.60c 2.5034E-04 26054.60c 6.7276E-04 26056.60c 1.0561E-02 &
  26057.60c 2.4390E-04 26058.60c 3.2458E-05 28058.60c 1.0103E-03 &
  28060.60c 3.8918E-04 28061.60c 1.6919E-05 28062.60c 5.3932E-05 &
  28064.60c 1.3743E-05 92235.60c 1.0642E-03 92238.60c 6.5656E-03 &
   8016.60c 1.3199E-02
m2 1001.60c 1.5820E-05 11023.60c 6.5728E-03  6000.60c 3.0195E-04 &
  13027.60c 5.0196E-03 22000.60c 1.1997E-04 24050.60c 1.3690E-04 &
  24052.60c 2.6399E-03 24053.60c 2.9935E-04 24054.60c 7.4514E-05 &
  25055.60c 2.4850E-04 26054.60c 6.7025E-04 26056.60c 1.0521E-02 &
  26057.60c 2.4299E-04 26058.60c 3.2337E-05 28058.60c 1.0029E-03 &
  28060.60c 3.8632E-04 28061.60c 1.6794E-05 28062.60c 5.3536E-05 &
  28064.60c 1.3642E-05 92235.60c 1.2222E-03 92238.60c 6.8447E-03 &
   8016.60c 1.3282E-02
m3 1001.60c 5.0247E-06 11023.60c 6.2598E-03  6000.60c 4.0190E-04 &
  13027.60c 2.4161E-03 22000.60c 1.3688E-04 25055.60c 2.8976E-04 &
  92235.60c 1.4786E-03 92238.60c 6.7585E-03  8016.60c 1.3240E-02 &
  24050.60c 1.5794E-04 24052.60c 3.0456E-03 24053.60c 3.4535E-04 &
  24054.60c 8.5965E-05 26054.60c 7.6967E-04 26056.60c 1.2082E-02 &
  26057.60c 2.7903E-04 26058.60c 3.7134E-05 28058.60c 1.1585E-03 &
  28060.60c 4.4624E-04 28061.60c 1.9399E-05 28062.60c 6.1840E-05 &
  28064.60c 1.5758E-05
m4 1001.60c 5.4267E-06 11023.60c 5.6338E-03  6000.60c 4.2824E-04 &
  13027.60c 2.5889E-03 22000.60c 1.3838E-04 25055.60c 2.9177E-04 &
```

```
  92235.60c 2.9720E-05 92238.60c 7.1145E-03  8016.60c 1.4299E-02 &
  94239.60c 1.4501E-03 94240.60c 7.0234E-05 94241.60c 8.0423E-07 &
  95241.60c 2.9419E-06 31000.60c 8.7691E-05 24050.60c 1.6073E-04 &
  24052.60c 3.0996E-03 24053.60c 3.5147E-04 24054.60c 8.7488E-05 &
  26054.60c 7.8381E-04 26056.60c 1.2304E-02 26057.60c 2.8416E-04 &
  26058.60c 3.7816E-05 28058.60c 1.1775E-03 28060.60c 4.5358E-04 &
  28061.60c 1.9719E-05 28062.60c 6.2857E-05 28064.60c 1.6017E-05
m5 1001.60c 1.0623E-05 11023.60c 5.6338E-03  6000.60c 3.6591E-04 &
  13027.60c 4.0036E-03 22000.60c 1.3132E-04 25055.60c 2.7457E-04 &
  92235.60c 1.8646E-03 92238.60c 7.0132E-03  8016.60c 1.4148E-02 &
  24050.60c 1.4974E-04 24052.60c 2.8875E-03 24053.60c 3.2742E-04 &
  24054.60c 8.1503E-05 26054.60c 7.3138E-04 26056.60c 1.1481E-02 &
  26057.60c 2.6515E-04 26058.60c 3.5287E-05 28058.60c 1.0983E-03 &
  28060.60c 4.2306E-04 28061.60c 1.8392E-05 28062.60c 5.8627E-05 &
  28064.60c 1.4939E-05
m6 6000.60c 2.4180E-04 13027.60c 9.1493E-04 22000.60c 3.7607E-04 &
  25055.60c 7.9296E-04 24050.60c 4.3685E-04 24052.60c 8.4241E-03 &
  24053.60c 9.5523E-04 24054.60c 2.3778E-04 26054.60c 2.1104E-03 &
  26056.60c 3.3129E-02 26057.60c 7.6509E-04 26058.60c 1.0182E-04 &
  28058.60c 3.2003E-03 28060.60c 1.2327E-03 28061.60c 5.3591E-05 &
  28062.60c 1.7083E-04 28064.60c 4.3531E-05
m7 6000.60c 1.1414E-02 13027.60c 1.0477E-04 22000.60c 4.3066E-05 &
  25055.60c 9.0806E-05  5010.60c 9.0632E-03  5011.60c 3.6481E-02 &
  24050.60c 5.0024E-05 24052.60c 9.6466E-04 24053.60c 1.0939E-04 &
  24054.60c 2.7228E-05 26054.60c 2.4167E-04 26056.60c 3.7938E-03 &
  26057.60c 8.7614E-05 26058.60c 1.1660E-05 28058.60c 3.6649E-04 &
  28060.60c 1.4117E-04 28061.60c 6.1371E-06 28062.60c 1.9563E-05 &
  28064.60c 4.9850E-06
m8 1001.60c 1.0700E-05  6000.60c 6.9662E-04 13027.60c 4.5454E-03 &
  22000.60c 4.3066E-05 25055.60c 9.0806E-05 92235.60c 5.8599E-05 &
  92238.60c 1.4028E-02  8016.60c 2.8194E-02 24050.60c 5.0024E-05 &
  24052.60c 9.6466E-04 24053.60c 1.0939E-04 24054.60c 2.7228E-05 &
  26054.60c 2.5609E-04 26056.60c 4.0200E-03 26057.60c 9.2840E-05 &
  26058.60c 1.2355E-05 28058.60c 3.6649E-04 28060.60c 1.4117E-04 &
  28061.60c 6.1371E-06 28062.60c 1.9563E-05 28064.60c 4.9850E-06
m9 1001.60c 2.4569E-04 11023.60c 5.5007E-03  6000.60c 4.9780E-04 &
  13027.60c 3.1458E-03 22000.60c 8.6518E-05 25055.60c 1.8243E-04 &
  92235.60c 3.8735E-05 92238.60c 9.2725E-03  8016.60c 1.8636E-02 &
  24050.60c 1.0050E-04 24052.60c 1.9380E-03 24053.60c 2.1976E-04 &
  24054.60c 5.4702E-05 26054.60c 4.9504E-04 26056.60c 7.7711E-03 &
  26057.60c 1.7947E-04 26058.60c 2.3884E-05 28058.60c 7.3625E-04 &
  28060.60c 2.8360E-04 28061.60c 1.2329E-05 28062.60c 3.9302E-05 &
  28064.60c 1.0015E-05
m10 1001.60c 7.0993E-06 11023.60c 5.5276E-03  6000.60c 4.9949E-04 &
  13027.60c 3.1570E-03 22000.60c 8.6577E-05 25055.60c 1.8255E-04 &
  92235.60c 3.8880E-05 92238.60c 9.3072E-03  8016.60c 1.8706E-02 &
  24050.60c 1.0057E-04 24052.60c 1.9394E-03 24053.60c 2.1991E-04 &
  24054.60c 5.4740E-05 26054.60c 4.9541E-04 26056.60c 7.7769E-03 &
  26057.60c 1.7960E-04 26058.60c 2.3902E-05 28058.60c 7.3673E-04 &
  28060.60c 2.8379E-04 28061.60c 1.2337E-05 28062.60c 3.9327E-05 &
  28064.60c 1.0021E-05
m11 1001.60c 3.5320E-04 11023.60c 8.1420E-03  6000.60c 2.0820E-04 &
  13027.60c 7.8779E-04 22000.60c 3.2381E-04 25055.60c 6.8278E-04 &
  24050.60c 3.7614E-04 24052.60c 7.2535E-03 24053.60c 8.2249E-04 &
  24054.60c 2.0474E-04 26054.60c 1.8172E-03 26056.60c 2.8525E-02 &
  26057.60c 6.5878E-04 26058.60c 8.7671E-05 28058.60c 2.7556E-03 &
  28060.60c 1.0615E-03 28061.60c 4.6145E-05 28062.60c 1.4710E-04 &
  28064.60c 3.7483E-05
m12 11023.60c 1.0936E-02  6000.60c 1.6468E-04 13027.60c 6.2311E-04 &
  22000.60c 2.5612E-04 25055.60c 5.4004E-04 24050.60c 2.9751E-04 &
  24052.60c 5.7372E-03 24053.60c 6.5055E-04 24054.60c 1.6194E-04 &
```

```
  26054.60c 1.4373E-03 26056.60c 2.2562E-02 26057.60c 5.2106E-04 &
  26058.60c 6.9344E-05 28058.60c 2.1796E-03 28060.60c 8.3956E-04 &
  28061.60c 3.6498E-05 28062.60c 1.1635E-04 28064.60c 2.9647E-05
m13 11023.60c 9.8043E-03  6000.60c 6.0934E-03 13027.60c 2.4029E-04 &
  22000.60c 9.8771E-05 25055.60c 2.0826E-04  5010.60c 4.8000E-03 &
   5011.60c 1.9320E-02 24050.60c 1.1473E-04 24052.60c 2.2124E-03 &
  24053.60c 2.5087E-04 24054.60c 6.2448E-05 26054.60c 5.5427E-04 &
  26056.60c 8.7008E-03 26057.60c 2.0094E-04 26058.60c 2.6741E-05 &
  28058.60c 8.4055E-04 28060.60c 3.2378E-04 28061.60c 1.4076E-05 &
  28062.60c 4.4869E-05 28064.60c 1.1433E-05
m14 6000.60c 9.2259E-05 13027.60c 3.4909E-04 22000.60c 1.4349E-04 &
  25055.60c 3.0256E-04 24050.60c 1.6668E-04 24052.60c 3.2142E-03 &
  24053.60c 3.6447E-04 24054.60c 9.0724E-05 26054.60c 8.0521E-04 &
  26056.60c 1.2640E-02 26057.60c 2.9191E-04 26058.60c 3.8848E-05 &
  28058.60c 1.2211E-03 28060.60c 4.7036E-04 28061.60c 2.0448E-05 &
  28062.60c 6.5183E-05 28064.60c 1.6610E-05
m15 6000.60c 1.5003E-02 13027.60c 1.7229E-04 22000.60c 7.0817E-05 &
  25055.60c 1.4932E-04  5010.60c 1.1907E-02  5011.60c 4.7925E-02 &
  24050.60c 8.2260E-05 24052.60c 1.5863E-03 24053.60c 1.7987E-04 &
  24054.60c 4.4774E-05 26054.60c 3.9740E-04 26056.60c 6.2384E-03 &
  26057.60c 1.4407E-04 26058.60c 1.9173E-05 28058.60c 6.0264E-04 &
  28060.60c 2.3213E-04 28061.60c 1.0092E-05 28062.60c 3.2169E-05 &
  28064.60c 8.1972E-06
m16 6000.60c 4.5532E-05 13027.60c 1.7229E-04 22000.60c 7.0817E-05 &
  25055.60c 1.4932E-04 24050.60c 8.2260E-05 24052.60c 1.5863E-03 &
  24053.60c 1.7987E-04 24054.60c 4.4774E-05 26054.60c 3.9740E-04 &
  26056.60c 6.2384E-03 26057.60c 1.4407E-04 26058.60c 1.9173E-05 &
  28058.60c 6.0264E-04 28060.60c 2.3213E-04 28061.60c 1.0092E-05 &
  28062.60c 3.2169E-05 28064.60c 8.1972E-06
m17 92235.60c 1.
m18 92238.60c 1.
m19 94239.60c 1.
kcode 6000 1 10 16010
ksrc 0. 0. 112.305
prdmp 3j 1
f4:n   35 36 37 38 39 40 41 42 43 44 45 46 47 48 49
f14:n  35 36 37 38 39 40 41 42 43 44 45 46 47 48 49
fm14    (1 17 -6) (1 18 -6) (1 19 -6)
print
```